Role of rift structural inheritance in orogeny highlighted by the Western Pyrenees case-study

Júlia Gómez-Romeu[1], Emmanuel Masini[2], Julie Tugend[2,3], Maxime Ducoux[2,4] & Nick Kusznir[1]

[1]Department of Earth, Ocean and Ecological Sciences, University of Liverpool, Liverpool, UK
[2]Total SA, R&D, Pau, France
[3]Sorbonne Université, CNRS-INSU, Institut des Sciences de la Terre, Paris, France
[4]E2S-UPPA, Université de Pau et Pays Adour-CNRS-TOTAL, LFCR IPRA, UMR 5150, Pau, France

Abstract

It is commonly accepted that many orogens form by contractional reactivation of earlier continental rifts or rifted margins. Therefore, to better understand orogenesis, it is important to also understand how rift domains and their associated structures are incorporated into orogens.

We investigate the role of rift structural inheritance during orogeny using the Western Pyrenees as a case-study. To achieve our aim, we use a kinematic forward lithosphere deformation model (RIFTER) to produce flexural isostatically compensated as well as balanced cross-sections showing the structural and stratigraphic development of both the rift and orogenic stages of the Western Pyrenees. The cross-section produced extends from the Northern to the Southern Foreland Basins and crosses the Mauléon-Arzacq Basin.

Our modelling results show how rift-domains and their faults are sequentially reactivated and incorporated into the present-day Western Pyrenees architecture. Based on the results from our case-study, we identify a sequence of tectonic stages separated by critical events that record the transition between different tectonic styles by which lithosphere is deformed. The pre-orogenic extensional stage is characterized by a hyper-extended rift system that eventually led to exhumed mantle. This constitutes the pre-orogenic template. The subsequent contractional tectonics consists of two stages: (i) the inversion of the hyper-extended rift system reactivating extensional structures and (ii) the crustal shortening of the southern proximal rift domain.

Results of the Western Pyrenees case-study may be used to understand the development of other Alpine-type collisional systems involving the sequential reactivation and inversion of former hyper-extended rift systems.

1. Introduction

The Wilson cycle represents one of the most important concepts of the plate tectonic theory and one of its key implications is that mountain belts are built on the former site of continental rifted margins (Wilson, 1966). This implies that present-day orogens are formed by the closure of precursor rift basins or rifted margins. Many studies have shown that remnants of distal rifted margins are present within internal parts of orogens (e.g. Alps: Lemoine et al., 1987; Manatschal, 2004; Mohn et al., 2010; 2014; Masini et al., 2012, Beltrando et al., 2014 and Epin et al., 2017, Pyrenees: Lagabrielle and Bodinier, 2008; Jammes et al., 2009; Lagabrielle et al., 2010; Clerc et al., 2012; Clerc and Lagabrielle, 2014, Masini et al., 2014, Tugend et al., 2014, Mouthereau et al., 2014, Teixell et al., 2016 and 2018, Caledonides: Andersen et al., 2012). These observations demonstrate the necessity of understanding the role of the earlier extensional rift history during orogen formation.

We use the Western Pyrenees as a natural laboratory to study the influence of rift structural inheritance on collision. The Western Pyrenees underwent Late Jurassic to Cretaceous rifting (Canérot, 2008; Jammes et al., 2009, 2010a) followed by the Alpine orogeny between the Santonian and the Miocene (Garrido-Megías and Ríos, 1972; Muñoz, 1992; Vergés et al., 1995; Capote et al., 2002; Vergés and García-Senz, 2001; McClay et al., 2004; Mouthereau et al., 2014). The contractional reactivation of the Western Pyrenees enabled the partial preservation of the earlier rift history (e.g. Jammes et al., 2009; Masini et al., 2014; Tugend et al., 2014). Tugend et al., (2014) has proposed that the sequential rift domain reactivation made a large contribution to the present-day orogen architecture of the Western Pyrenees making it an ideal case-study to study the role of rift structural inheritance during orogeny. We investigate the sequential rift domain reactivation paying particular attention to the role of pre-existing rift structures required to produce the present-day Western Pyrenees architecture.

Early work showing balanced geological sections across the Pyrenees (e.g. Roure et al., 1989; Choukroune et al., 1990; Muñoz, 1992; Teixell, 1998; Vergés et al., 2002) used pull-apart basins as the initial template for the collisional stage. However, recent published cross-sections (Jammes et al., 2009; Tugend et al., 2014; Mouthereau et al., 2014; Teixell et al., 2016) have improved the pre-orogenic template by including a hyper-extended rift architecture, consistent with observations of major crustal thinning and mantle exhumation (Lagabrielle and Bodinier, 2008; Jammes et al., 2009; Lagabrielle et al., 2010; Masini et al., 2014; Tugend et al., 2014, 2015b). A common feature of all these sections is that they are palinspastically restored but do not include the flexural isostatic compensation of the lithosphere resulting from both extensional and contractional tectonics. In this study, we use a kinematic forward lithosphere deformation model (RIFTER) that allows us to produce flexural isostatically compensated as well as balanced cross-sections.

Using RIFTER we produce a cross-section extending from the Northern (Aquitaine Basin) to the Southern Foreland Basins, that crosses the Mauléon-Arzacq Basin, and incorporates both the hyper-extended rifting and the orogenic evolution of the Western Pyrenees. Our modelling strategy consists of bringing together the shallow observed geology, seismic reflection observations and the deeper seismic tomographic structure of the Western Pyrenees into a single unified model that balances isostatically as well as structurally. Our RIFTER modelling shows that by including the earlier rift history we are able to reproduce the present-day first-order structural and stratigraphic architecture of the Western Pyrenees. We show that the present-day first-order structure of this orogen can be reproduced through the sequential reactivation of pre-existing rift domains. In addition, we bring insights on how the pre-orogenic rift-related faults may be reactivated and incorporated into the present-day Western Pyrenees architecture.

2. Geological setting

The Pyrenees is a double vergent orogen orientated east-west and located at the boundary between Spain (part of the Iberian plate) and France (part of the European plate). It is bounded to the east by the Mediterranean Sea and to the west by the Bay of Biscay (Figure 1). The Pyrenees form the central part of an orogenic system, developed subsequently to the subduction of the Iberian plate underneath the European plate.

2.1. Present-day structure of the Pyrenees

The Pyrenees can be divided into five main structural units. From north to south these are: (1) the Aquitaine Northern Foreland Basin, (2) the North Pyrenean Zone forming the retro-wedge of the orogen where Meso-Cenozoic rocks are exposed, (3) the Axial Zone made by a stack of thrust sheets involving Paleozoic basement, (4) the South

Pyrenean Zone forming the pro-wedge of the orogen and (5) the Ebro Foreland Basin (e.g. Choukroune and Séguret, 1973; Mattauer and Henry, 1974; Teixell, 1990; Daignières et al., 1994 and references therein) (Figure 2a). In the eastern and central part of the Pyrenees, the Axial Zone is well-developed exposing Palaeozoic rocks (Figure 2a). Towards the west, the Axial Zone is reduced and the Mauléon Basin, made up of Mesozoic sediments, occupies most of the western edge of the Pyrenees (Figure 2a). In the northern and southern part of the Pyrenees, a wide range of sediments ranging from Lower Triassic up to Lower Miocene are present (Figure 2a). It is important to highlight the presence of an evaporitic sequence at the bottom of the Mesozoic cover (Upper Triassic) that acts as a decollement layer and strongly controls both the extensional and compressional tectonics of the Pyrenees (Canérot, 1989; James and Canérot, 1999; Jammes et al., 2010b; Lagabrielle et al., 2010). The Aquitaine Northern and Ebro Southern Foreland Basins contain Neogene sediments deposited during the syn- to post-orogenic evolution of the Pyrenees (Figure 2a) (see Vacherat et al., 2017 and Grool et al., 2018 for a detailed tectonostratigraphy of these basins).

During the Alpine collision, the Pyrenees orogen was mainly deformed by E-W trending thrust faults such as the North Pyrenean Frontal Thrust and the South Pyrenean Frontal Thrust (Figure 2a). Additionally, present-day NE-SW trending faults (e.g. Toulouse structure) that formed in the Late Variscan (Burg, 1994) were possibly partly reactivated as transfer zones during rifting (Tugend et al., 2014). What type of Variscan faults they were and how they reactivated during the development of the Pyrenees remains uncertain.

2.2. Tectonic evolution of the Pyrenees

The opening of the North Atlantic Ocean together with the opening of the Bay of Biscay strongly controlled the relative motions of the Iberian plate with respect to the European and African plates (e.g. Olivet, 1996; Rosenbaum et al., 2002; Macchiavelli et al., 2017; Nirrengarten et al., 2018). The relative movements between these three plates are recorded through the tectonic evolution of the Pyrenees. Over the past 30 years, the formation and development of the Pyrenees have been intensively studied (e.g. Le Pichon et al., 1971; Srivastava et al., 1990; Roest and Srivastava, 1991; Sibuet and Collette, 1991; Olivet, 1996), but there is still controversies on the paleogeographic evolution prior to the Alpine collision of this orogen. As a first order simplification, the

Pyrenees can be considered as the result of several extensional and compressional tectonic events that initiated in the Palaeozoic and finalized in the Miocene. We focus on the main rift episode that occurred from latest Jurassic to early Late Cretaceous time (Schettino and Scotese, 2002; Canérot, 2008; Jammes et al., 2009, 2010a; Tugend et al., 2015b). The rifting episode was followed by the Alpine orogeny that took place between the Late Santonian and the Miocene (Garrido-Megías and Ríos, 1972; Muñoz, 1992; Vergés et al., 1995; Capote et al., 2002; Vergés and García-Senz, 2001; McClay et al., 2004; Mouthereau et al., 2014).

2.2.1. Rift evolution

The pre-Alpine evolution of the Iberian and European plate boundary was accommodated within three oblique rift systems; the Bay of Biscay-Parentis, the Pyrenean-Basque-Cantabrian and the Central Iberian Range (Salas and Casas, 1993; Vergés and García-Senz, 2001; Roca et al., 2011; Tugend et al., 2014; 2015a). The onset of the Mesozoic rifting occurred in the latest Jurassic (Figure 3a) during an overall left-lateral movement between the Iberian and European plates deduced from plate kinematic scenarios (e.g. Rosenbaum et al., 2002; Schettino and Scotese, 2002; Canérot, 2008; Jammes et al., 2010a; Nirrengarten et al., 2018). Details of the partitioning of the deformation between the different rift systems remain debated (Tugend et al., 2015a; Nirrengarten et al., 2018; Rat et al., 2019). From the Aptian up to early Late Cretaceous the relative movement between Iberia and Europe appears purely divergent as deduced from field interpretations (Jammes et al., 2010a; Tavani et al., 2018). Onset of sea-floor spreading of the western Bay of Biscay in Aptian time (Montadert et al., 1979) (Figure 3b) coincides with the main crustal thinning event and local mantle exhumation in the Pyrenean-Basque-Cantabrian rift system (Lagabrielle and Bodinier, 2008; Jammes et al., 2009; Masini et al., 2014; Tugend et al., 2014; 2015b) (Figure 3c). The identification of anomaly 34 in the Bay of Biscay and absence of anomaly 33 (Roest and Srivastava, 1991) suggest that sea-floor spreading persisted until Santonian-Early Campanian time (e.g. Montadert and Roberts, 1979, Montadert et al., 1979). This extensional deformation is not evidenced in the Pyrenean-Basque-Cantabrian rift system.

The relative movement between the Iberian and European plates resulted in a complex rift domain architecture giving the pre-Alpine setting of the Pyrenees (Figure 3c).

2.2.2. Convergence evolution

Onset of the Alpine orogeny (Figure 3d) started in the late Santonian – Campanian (Garrido-Megías and Ríos 1972; Capote et al., 2002; McClay et al., 2004) and evolved up to the Late Oligocene – Early Miocene (Muñoz, 2002; Verges et al., 2002). This orogeny is related to the northward motion of Africa relative to Europe (e.g. Rosenbaum et al., 2002) leading to a north-south to northeast-southwest convergent motion between the Iberian and European plates. In the Pyrenees, this motion is characterized by the subduction of Iberia beneath Europe (Pulgar et al., 1996; Gallastegui et al., 2002; Muñoz, 1992, 2002; Pedreira et al., 2007). During this episode, Mesozoic basins were shortened and inverted leading to the formation of the present-day architecture of the Pyrenees (Capote et al., 2002).

3. Modelling constraints for the Western Pyrenees

Our modelled section includes both the Northern and the Southern Foreland Basins but we pay particular attention to the Arzacq-Mauléon Basin development. This basin initially formed during rifting and was later reactivated during the Alpine orogeny. A singular feature of this basin is that it escaped from most of the pervasive Alpine deformation and exposes part of the pre-collision history (e.g. Jammes et al., 2009; Masini et al., 2014).. We have less constraints for the rifting episode along the rest of the section but we use the available dataset to infer the rift record and how this may have been reactivated during collision.

Our modelling strategy consists of bringing together the shallow observed geology, seismic observations and the deeper structure of the Western Pyrenees into a single unified model that balances isostatically as well as structurally. In particular, we use sub-surface geology (down to a depth of 5-10 km) along the eastern Mauléon Basin (Figure 4a-c) and the deep crustal structure along the western Mauléon Basin (Figure 4d). The sub-surface observations for the Southern Foreland Basin (i.e. Ebro and Jaca Basins), the Axial Zone and the Mauléon Basin are based on the work by Teixell et al., (2016 and 2018), Tugend et al., (2014) and Lagabrielle et al., (2010) respectively (Figures 4a-b). The architecture of the Aquitaine-Arzacq Basin (Figure 4c) is revealed by the interpretation of seismic reflection line nº1325 (Appendix 1) together with well data owned by Total SA. Because no deep crustal information is available across the eastern Mauléon Basin, we use first-order deep constraints from the western Mauléon

Basin. These are obtained from a passive seismic tomography transect (PYROPE, Wang et al., 2016; Chevrot et al., 2018), whose data was acquired by Chevrot et al., (2015) and are shown in Figures 4d-e.

The RIFTER model is used to bring together sub-surface and deep observations distributed across the Western Pyrenees into a single unified model that balances isostatically as well as structurally, showing both the rifting and convergent evolution of this orogen.

3.1. Sub-surface geology

From south to north, the transect that we model consists of the sub-surface geology of; the Southern Foreland Basin, Axial Zone, Mauléon Basin, Grand Rieu Ridge and the Arzacq Basin (e.g. Casteras, 1969; BRGM, 1974; Le Pochat et al., 1976; Teixell, 1990; Daignières et al., 1994; Serrano et al., 2006; Jammes et al., 2009; Masini et al., 2014).

Southern Foreland Basin

The Southern Foreland Basin (i.e. Jaca and Ebro basins) formed as a consequence of the Axial Zone loading leading to the flexure of the Iberian lithosphere as compressional deformation was migrating southwards. Most of the calciclastic and siliciclastic sedimentation that fills up this basin is derived from the erosion of the Axial Zone during the Cenozoic. The South Pyrenean Frontal Thrusts affects the sedimentary cover of the Southern Foreland Basin leading to the last compressional deformation by early Miocene times (Teixell et al., 2016) (Figure 4a).

Axial Zone

One of the key characteristics of the Axial Zone is the deposition of post-rift sediments (Turonian and younger) on top of the eroded basement due to the occurrence of a major hiatus (Jammes et al., 2009; Masini et al., 2014) (Figures a-b). This hiatus argues for a major uplift and/or no deposition on the future Axial Zone during the rifting episode (Jammes et al., 2009). The Gavarnie and Guarga north-dipping thrusts are the main structures that led to the uplifting of the Axial Zone during the Late Cretaceous and Cenozoic Pyrenean collision. The overall timing of these structures is well documented by tectono-sedimentary and thermochronological data (e.g. Teixell et al., 2016 and references therein). However, the Gavarnie and Guarga thrust geometries at depth remains poorly understood as does their importance in terms of shortening (e.g.

Cochelin et al., 2018).

Mauléon Basin

Former rift structures are exposed and preserved in the western Mauléon Basin enabling extensive studies of basement-sediment primary relationships (e.g. Jammes et al., 2009; Masini et al., 2014; Tugend et al., 2015b; Saspiturry et al., 2019). While preservation of these rift structures along the eastern Mauléon Basin is poor, former structural rift domains can still be identified and correlated at the scale of the entire basin (Tugend et al., 2015b).

The Mauléon Basin is squashed between the Grand Rieu Ridge to the north and the Axial Zone to the south (Lagabrielle et al., 2010; Masini et al., 2014; Tugend et al. 2014; Teixell et al., 2016) by the NPFT and the Lakhora Thrust system respectively (Figures 4b-c). A remarkable feature of this basin is that it preserves a complex rift history showing discontinuous pre-rift layers lying on top of the Upper Triassic evaporitic decollement as well as a non-uniform syn-rift sedimentary architecture (Masini et al., 2014) (Figure 4b). Studies carried out in the Mauléon Basin (e.g., Jammes et al., 2009; Lagabrielle et al., 2010; Masini et al., 2014; Tugend et al., 2014) suggest that it was formed through a hyper-extension rift episode leading to extreme crustal thinning and mantle exhumation. Field studies such as Masini et al., (2014) interpreted that this deformation was accommodated by two diachronous thick-skinned detachment systems (the Southern Mauléon Detachment and the Northern Mauléon Detachment) related to the formation of two sub-basins; the Southern Mauléon Basin and the Northern Mauléon Basin respectively. The onset of the tectonic inversion of the Mauléon Basin occurred between Santonian and Campanian times (Teixell et al., 2016 and references therein). This inversion episode led to the thrusting of the Northern Mauléon Basin over the former Grand Rieu Ridge and Arzacq Basin (e.g. Casteras, 1969; Teixell, 1990 and 1998; Muñoz, 1992; Daignières et al., 1994) while the Southern Mauléon Basin was thrusted over the Axial Zone along the Lakhora Thrust system (Muñoz, 1992; Teixell, 1998). The presence of south-directed thrust sheets made of Mauléon Basin sediments within the former hyper-extended domain and subsequently folded and tilted during the formation of the Axial Zone located to the south, argues that the Alpine shortening began in the hyper-extended basin by Cretaceous times before migrating into the Axial Zone by Eocene times (Tugend et al., 2014; Dumont et al., 2015).

Grand Rieu Ridge

The Grand Rieu Ridge is characterized by the local absence of syn-rift sediments (e.g. Cardesse 2 drill hole; Serrano et al., 2006; Tugend et al., 2014). Post-rift sediments cover either discontinuous slivers of pre-rift cover or lay directly on top of basement (Masini et al., 2014) (Figure 4c). The north-vergent North Pyrenean Frontal Thrust system is located on this ridge that separates the Arzacq Basin in the north from the Mauléon Basin in the south (Figures 4b-c).

Arzacq Basin

The architecture of the Arzacq Basin (Figure 4c) is revealed using the seismic reflection line nº1325 (Appendix 1) together with well data owned by Total SA. It consists of a smooth 25 km wide “sag basin” syncline consisting of sediments of Permian-Lower Triassic to Quaternary age. A north-dipping extensional fault is the main observed rift structure, which bounds the southern Arzacq Basin and separates it from the Grand Rieu Ridge basement. On top of this major fault, syn-rift sediments (Aptian-Albian in age) show a growth strata development in an overall syncline-shape geometry. This indicates that the deformation of the basement was decoupled from the sedimentary cover by a major basal decollement level corresponding to the Triassic Keuper evaporitic layer (e.g. Le Pochat et al., 1978; Canérot et al., 2001; Jammes et al., 2010b; Masini et al., 2014). It can be inferred that the pre-tectonic sedimentary cover lying above the Upper Triassic decollement was dragged and gently folded above the normal fault. No important collisional structures can be identified within this basin at this location apart from a few thrusts at the southern edge of the Arzacq Basin corresponding to the North Pyrenean Frontal Thrust system (Figure 4c) suggesting that a minor compressional tightening affected this basin (see Rocher et al., 2000 for a detailed structural analysis of this basin). The Arzacq Basin is characterized by substantial crustal thinning reaching beta values of 2 (Brunet, 1984) and consistent with the crustal architecture imaged by Wang et al., (2016). Indeed, the overall subsidence evolution of this basin can only be explained by a post-rift thermal subsidence continuing largely after the onset of shortening (Angrand et al., 2018). Masini et al., (2014) pointed out that the amount of thinning that the Arzacq Basin underwent cannot be simply provided by the observed north-dipping extensional fault located at the southern edge of the basin. They suggested that additional thinning may have been achieved by strain transfer from the Southern Mauléon Detachment in the Southern Mauléon Basin to the middle and lower crustal levels in the Arzacq Basin. This crustal decoupling structure may have generated the asymmetric rifting architecture between the Mauléon Basin (lower plate) and the Arzacq Basin (upper plate).

3.2. Deep crustal structure

Recent studies have imaged the deepest part of the Western Pyrenees, along the western Mauléon Basin, based on a tomographic model (Chevrot et al., 2015 and 2018; Wang et al., 2016). Figure 4d shows the Vs seismic velocity model obtained by full waveform inversion together with a simple interpretation of the crustal architecture suggested by Wang et al., (2016). The Vs data shows the southernmost Iberian Moho at 30 km depth which gently dips to the north reaching 50 km deep beneath the Mauléon Basin. In contrast, the geometry of the European Moho is almost horizontal beneath the Arzacq Basin at 30 km deep while beneath the Mauléon Basin it becomes shallower reaching 10 km depth. Indeed, in the western part of the Mauléon Basin, a strong positive Bouguer gravity anomaly is observed (Figure 4e) and has been interpreted as deriving from a piece of Iberian mantle (Casas et al., 1997; Jammes et al., 2010a) or lower crust (Grandjean, 1994; Vacher and Souriau, 2001; Pedreira et al., 2007). However, the work by Wang et al., (2016) shows seismic velocities beneath the western part of the Mauléon Basin (Vp ~ 7.3 km/s and Vs 4.2 km/s) that were interpreted as a body of exhumed mantle, inherited from the pre-collision hyperextended rift system. These geophysical results are consistent with many recent geological studies of the Western Pyrenees that describe remnants of a hyper-extended rift with pre-orogenic mantle exposures (e.g., Jammes et al., 2009; Lagabrielle et al., 2010; Masini et al., 2014; Tugend et al., 2014; Tugend et al., 2015b). We use the Iberian Moho geometry as well as the geometry of the European indenter as reference observations to constrain our modelled profile. The disappearance of the main gravity anomaly towards the eastern Mauléon Basin (Figure 4e) suggests that, if the mantle body exists, then it would be of limited importance under the eastern Mauléon Basin or consist of less-dense more intensively serpentinized mantle. Masini et al., (2014) suggested that this difference in gravity anomaly between the western and eastern Mauléon Basin (Figure 4e) may result from a lateral change in the Pyrenean structure accommodated by the Saison transverse structure.

3.3. Rift domains

The repartition of former rift domains in the present-day Pyrenean orogen was recently interpreted by Tugend et al., (2014) (Figure 3e). At the scale of the Western Pyrenees, the Arzacq Basin likely recorded the necking of the European plate in an upper plate setting bounded in the south by the Northern Mauléon Detachment (Masini et al., 2014). The Northern Mauléon Basin presumably corresponded to a lower plate hyper-extended domain including (the hyperthinned and exhumed mantle domains in Tugend et al., 2014. The Southern Mauléon Basin is interpreted as the former Iberian necking domain while the former proximal domain might be eroded in the Axial Zone or buried beneath the southern Pyrenees (Figure 3e).

4. RIFTER model

We use a numerical model (RIFTER) to constrain the evolution of the Western Pyrenees. RIFTER is a kinematic forward lithosphere deformation model that allows the production of flexural isostatically compensated as well as balanced cross-sections. Within RIFTER, lithosphere is deformed by faulting in the upper crust with underlying distributed pure-shear deformation in the lower crust and mantle. A key attribute of RIFTER is that it incorporates the flexural isostatic response to extensional and/or reverse faulting, crustal thinning and/or thickening, lithosphere thermal loads, sedimentation and erosion. Therefore, RIFTER can be used to model and predict the structural and stratigraphic development of both extensional and contractional tectonic settings. The model is kinematically controlled with fault geometry and displacement, pure-shear distribution and the amount of sedimentation and erosion given as model inputs as a function of time. Lithosphere flexural strength, parameterised as lithosphere effective elastic thickness, is also defined. The model incorporates lithosphere thermal perturbation and re-equilibration in response to lithosphere deformation. Model outputs are geological cross-sections which are flexural isostatically compensated as well as structurally balanced. The kinematic formulation of RIFTER represents an advantage over dynamic modelling because the input data given to RIFTER can be constrained by observed geology. In addition RIFTER provides for the isostatic testing of palinspastic cross-sections and can also be used to explore different kinematic scenarios. A more detailed description of the model formulation (originally called OROGENY) is given by Toth et al., (1996), Ford et al., (1999) and Jacome et al., (2003). These studies show the model formulation applied to contractional tectonics however similar physical principles apply for an extensional tectonics scenario.

The fundamental behaviour of RIFTER and its flexural isostatic response, to sequential faulting, sedimentation and erosion, is shown in Figure 5 for both simple extensional and contractional settings. The upper lithosphere is deformed by faults whose geometry is assumed to be listric and whose response to fault displacement is calculated using the vertical shear (Chevron) construction. Faults within RIFTER detach at a defined horizontal level, below which the deeper lithosphere is deformed by pure-shear.

RIFTER also includes the deeper lithosphere deformation response during extensional and/or contractional tectonics. Failure to incorporate this deeper deformation results in an unrealistic cross-section, as shown in Figures 5a and 5f where an extensional and reverse fault respectively deform the upper lithosphere without any deep pure-shear deformation below. Any robust lithospheric model must include both the upper and lower lithosphere deformation response to extensional and/or contractional tectonics.

Model results shown in Figures 5b-e (for extension) and Figures 5g-j (for shortening) include deeper deformation and the flexural isostatic response to faulting, crustal thinning or thickening, sediment fill, erosion, lithosphere thermal perturbation and re-equilibration. Figure 5b shows half-graben formation resulting from a single extensional fault while Figure 5g shows subsidence and foreland basin formation ahead of the over-thrusting. For both extension and shortening, sediment fill and its isostatic loading generates subsidence while erosion consisting of unloading of the subaerial topography generate flexural uplift. New faults modify the earlier formed basins. For extensional tectonics, lithosphere thermal re-equilibration results in post-tectonic thermal subsidence (Figures 5c-e) while for shortening, re-equilibration results in thermal uplift (Figures 5h-j).

5. Modelling experiments applied to the Western Pyrenees

RIFTER model is used to construct the development of the Western Pyrenees across the hyper-extended Mauléon Basin including the Northern (Arzacq) and the Southern Foreland Basins. In this section, we present a set of sequential 2D crustal sections showing the rift and orogenic forward evolution of the Western Pyrenees (Figure 6).

5.1. Rifting evolution

Three main extensional events are responsible of the Arzacq-Mauléon Basin formation (Masini et al., 2014; Jammes et al., 2009). These are; (i) an early rifting event believed to be dominated by a left-lateral transtensional movement but currently highly debated (Late Jurassic – Early Cretaceous), (ii) a necking rifting event (Aptian–Albian) and (iii) a hyper-extended rifting event leading to extreme crustal thinning and locale mantle exhumation (Albian – Cenomanian). Because several studies highlighted the role of salt tectonics in this area (James and Canérot, 1999; Canérot, 1989; Jammes et al., 2010b; Lagabrielle et al., 2010; Masini et al., 2014), we tentatively include this in our modelling as a supplementary surface decollement. However, using our kinematic model, we are unable to generate diapiric structures arising from salt tectonics; this study focuses on the large crustal scale architecture.

Initial RIFTER model setup consists of horizontal layers with uniform thickness. From top to bottom they are; (i) 2 km of pre-rift sediments representing Upper Triassic to Lower Jurassic times, (ii) 28 km of continental crust representing basement consisting of pre-Triassic rocks, (iii) 90 km of continental lithospheric mantle and (iv) asthenospheric mantle.

5.1.1. Early rifting

The first extensional episode that we model is poorly constrained and understood. It has been suggested that during the Late Jurassic – Early Cretaceous a transtensional rifting episode may have occurred leading to slight crustal thinning (e.g. Jammes et al., 2009 and 2010a), however this is currently debated. Local erosion within Jurassic sediments together with Neocomian bauxitic deposits indicate sub-aerial exposures (e.g. James et al., 1996; Canérot, 2008). During the Late Jurassic – Early Cretaceous, the Aquitaine basin recorded long wavelength vertical motions (e.g. Brunet, 1984; Biteau et al., 2006) rather than an intense localized crustal stretching and thinning which suggests that this deformation might have been controlled by lithospheric scale processes. While Canérot (2008) proposed a regional "transpression" event, recent studies have shown that this phase is coeval with the main stage of transtensional rifting in the nearby Bay of Biscay westwards and Central Iberian Range rift system southwards, both acting as the limits of a diffuse plate boundary at this time (e.g. Tugend et al., 2015a; Nirrengarten et al., 2018; Tavani et al., 2018; Rat et al., 2019). Based on these studies, we suggest that the Late Jurassic – Early Cretaceous rifting episode in the Western Pyrenees occurred due to incipient crustal stretching and thinning ahead of the propagation tip of the Bay of Biscay.

We represent this episode in RIFTER by a non-uniform minor crustal thinning (15 km of extension) followed by partial erosion (Figures 6a and 7a). This deformation affects only the southern area of the model resulting in slight uplift and partial erosion of Upper Triassic to Lower Jurassic sediments which is consistent with field observations (Figure 2).

5.1.2. Necking rifting

The second modelled extensional episode corresponds to the necking rift event that occurred between the Aptian and Albian (Jammes et al., 2009; Masini et al., 2014). The deformation that resulted from this episode is believed to be achieved by the Southern Mauléon Detachment system and an extensional fault that controls the formation of the Southern Mauléon Basin and the Arzacq Basin respectively (Masini et al., 2014). The activity of these north-directed extensional faults started in the Lower Aptian and lasted until the Lower Albian although the climax of the deformation took place between the Upper Aptian and the Lower Albian (Jammes et al., 2009; Masini et al., 2014; Tugend et al., 2014). Lower crustal thinning (boudinage) may have occurred during this stage and, in the Arzacq Basin which shows crustal thinning by a factor of 2 (e.g. Brunet, 1984), may have been more important than the upper crustal stretching.

To reproduce the consequences of the necking rifting episode, we develop a model template that shows asymmetric crustal thinning (37 km of total extension) affecting only the northern part of the model (Figure 6b). To achieve this, we first create two north-dipping extensional faults soling out at lower crustal levels followed by Lower Aptian sedimentation (Figure 7b). These structures form the northern realm of the Southern Mauléon Detachment and the extensional fault controlling the Arzacq Basin formation (i.e. South-Arzacq fault in this study), the displacement of which is achieved using the Triassic salt layer as a decoupling horizon. We then reactivate the northern realm of the Southern Mauléon Detachment and add another sedimentary unit equivalent to Middle Aptian times (Figure 7c). The last input parameter is the formation of the southern realm of the Southern Mauléon Detachment followed by Upper Aptian to Lower Albian sedimentation and 15 Myr of thermal subsidence representing the duration of the rift event (Figure 7d). As a result of these input parameters, smooth synclines, approximately 5 km deep, consisting of pre- and syn-necking rift sediments are predicted within the Southern Mauléon Basin and the Arzacq Basin (Figures 6b and 7d). These geometries are consistent with the structural observations from the Arzacq Basin (Figure 4c and Appendix 1) as well as with the outcropping of the southern part of the Mauléon Basin located ~20 km west of the cross-section shown in Figure 4b consisting of the Arbailles massif syn-rift syncline (Canérot, 2008). The resultant deep crustal architecture of the Southern Mauléon Basin is characterized by an important crustal thinning forming the typical crustal neck shape whereas beneath the Arzacq Basin the crustal thinning is less pronounced and mainly focused within the lower crust.

5.1.3. Hyper-extension rifting

The last extensional episode modelled corresponds to the hyper-extension rift event. According to Masini et al., (2014), major crustal thinning was achieved by the Northern Mauléon Detachment between Middle Albian and Cenomanian times. This deformation led to the Northern Mauléon Basin formation located between the Southern Mauléon Basin and the Grand Rieu Ridge.

To reproduce this extensional episode, we develop a model that gives major crustal thinning (30 km of total extension) together with mantle exhumation (Figure 6c). To achieve this, we create the Northern Mauléon Detachment corresponding to a large north-dipping extensional fault crosscutting the previously thinned continental crust and coupled into the mantle (Figure 7e) and the Future North Pyrenean Frontal Thrust consisting of an extensional antithetic conjugate fault of the Northern Mauléon Detachment (Figure 7f). The fact that the Northern Mauléon Detachment cuts through a previous necking decollement and thinned crust implies that the crust ahead of the breakaway zone of the Northern Mauléon Detachment is substantially thin. This is in accordance with observations from the western Mauléon Basin where a thinned crustal section without most of the middle-lower crustal rocks is reported (Labourd massif section, Jammes et al., 2009; Masini et al., 2014).

The displacement of the Future North Pyrenean Frontal Thrust (i.e. along the southern slope of the Grand Rieu Ridge) is achieved using the Triassic salt as a decoupling horizon mimicking gravity slides into the axis of the Mauléon Basin. In particular, this tectonic event allows the movement of pre- to syn-hyper-extension sediments from the southern flank of the Grand Rieu Ridge downwards in to the Northern Mauléon Basin.

We add a sedimentary unit (representing Middle-Albian to Cenomanian times) while deformation occurs followed by 15 Myr of thermal subsidence (Figure 7f). As a result of these input parameters, the Northern Mauléon Basin with its 8 km deep depocenter is formed together with the occurrence of crustal breakup and mantle exhumation (Figure 7f). The resultant crustal architecture of hyper-extension rifting is that of a typical young pair of conjugate rifted margins characterized by Iberia being the lower plate and Europe being the upper plate (Figure 6c).

5.2. Post-rifting

To reproduce the post-rifting stage, we first generate erosion followed by 8 Myr of thermal subsidence and partial sedimentation corresponding to post-rift sediments of Turonian to Coniacian age. As a result of this input data, regional subsidence is produced (Figure 6d).

Using RIFTER we have reproduced the development of the rift evolution of the Western Pyrenees (Figures 6a-c) using 82 km of total extension. This post-rifting stage (Figure 6d) is the initial template that we use for the subsequent collisional development of the Western Pyrenees.

5.3. Orogenic evolution

In this section, we quantitatively test a sequential reactivation of former rift domains leading to orogen formation using the Western Pyrenees case-study by reproducing the following three events; (i) reactivation of the hyper-extended domain, (ii) reactivation of the necking domain and (ii) shortening of the proximal domain.

5.3.1. Reactivation of hyper-extended domain

To reproduce the reactivation of the hyper-extended domain (i.e. the hyperthinned and exhumed mantle domains), we use RIFTER to generate a model that shows the nappe-stacking of the Northern Mauléon Basin sedimentary cover while the exhumed Iberian material is underthrusted below the Grand Rieu Ridge. This leads to the closure of the exhumed mantle domain and shortening of the hyper-thinned domain (Figure 6e) (Jammes et al., 2009; Mouthereau et al., 2014; Tugend et al., 2014; Dumont et al., 2015; Teixell et al., 2016). The structures related to this phase are affected by the later folding and thrusting collisional phase suggesting that the reactivation of the hyper-extended domain took place between the Santonian and Upper Cretaceous (Tugend et al., 2014; Dumont et al., 2015).

To achieve this collisional stage, we reactivate the Northern Mauléon Detachment and the North Pyrenean Frontal Thrust together with minor additional shortening generated by two new north-dipping synthetic thrusts of the Northern Mauléon Detachment leading to the Chaînons Béarnais formation (Figures 8a-b). We add sedimentation while the deformation occurs followed by 6 Myr of thermal re-equilibration and partial erosion. As a consequence of 19 km of shortening during the reactivation of the hyper-extended domain, an important uplift of the Northern Mauléon Basin sedimentary cover (e.g. Chaînons Béarnais fold and thrust belt) corresponding to an accretionary wedge is formed (Figure 6e).

5.3.2. Reactivation of necking domain

For the convergent reactivation of the necking domain, we use 52 km of shortening in RIFTER which generates sub-aerial regional uplift and leads to the restoration of crustal thickness to near normal (~30 km) (Figure 6f). This stage is mostly accommodated by south-directed thrusting along the Lakhora-Eaux Chaudes thrust system (Teixell, 1998; Tugend et al., 2014; Dumont et al., 2015; Teixell et al. 2016). Shortening in this domain occurs between the Late Cretaceous and Early Eocene, before the deformation migrates into the subsequent main structures of the Axial Zone (i.e. Gavarnie and Guarga thrusts). The transition between the pre- and post-Palaeocene shortening remains poorly constrained during the reactivation of the necking domain due to an erosional post-Cretaceous event (Bosch et al., 2016). The reactivation of the necking domain is partly simultaneous with the reactivation of the hyper-extended domain as well as with relief initiation in the Axial Zone (Teixell et al., 2016 and 2018). This indicates that the reactivation of the necking domain is a transitional phase consistent with recent results of thermo-mechanical modelling experiments (Jourdon et al., 2019).

To achieve the reactivation of the necking domain, we use the Southern Mauléon Detachment system, the Northern Mauléon Detachment, and the North Pyrenean Frontal Thrust consisting of an antithetic structure of the Southern Mauléon Detachment (Figures 8b-c). Note that the Northern Mauléon Detachment only acts as the underthrusting plane and therefore its shallower segment is not active. We first displace by thrusting a realm of the North Pyrenean Frontal Thrust and the southernmost realm of the Sothern Mauléon Detachment system (i.e. Lakhora Thrust), followed by partial erosion and sedimentation. The Lakhora Thrust consists of a synthetic footwall fault of the Northern Mauléon Detachment coupled into the shallow mantle enabling to carry upwards a small piece of mantle. We then thrust the northernmost realm of the Southern Mauléon Detachment system (i.e. a synthetic hangingwall fault of the Lakhora Thrust) followed by partial erosion and sedimentation. As a result of this tectonic event, the pop-up of the Southern Mauléon Basin and the Northern Mauléon Basin sedimentary cover is accomplished together with the development of the pre-indentation structure between the Iberian and European plates (Figure 6f). Note that as a consequence of this tectonic event a relatively small piece of anomalously shallow mantle is generated which is consistent with the attenuation of the gravity anomaly towards the east of the Mauléon Basin. In contrast with the western Mauléon Basin where a larger gravity anomaly is observed and interpreted as a shallow large mantle body (Wang et al., 2016). To sample and carry upwards a large piece of mantle, the Lakhora Thrust may has to be coupled into deeper mantle during the reactivation of the necking domain.

5.3.3. Shortening of proximal domain

The later collision phase is characterized by the formation of the Axial Zone together with the development of the Southern Foreland Basin (Figure 6g). This deformation phase occurred between the Eocene and Miocene times which corresponds to the climax of the Alpine orogeny of the Western Pyrenees. This phase is generally described as responsible for the creation of high relief and acceleration of crustal thickening in the Axial Zone and flexural subsidence in the foreland basin.

To reproduce this stage, we develop a set of new south-vergent thrusts crosscutting the Iberian unthinned crust (Figures 8d-e). These structures are, from north to south; Gavarnie Thrust, a minor thrust, Guarga Thrust, and the South Pyrenean Frontal Thrust (Lacombe and Bellahsen, 2016). Additional intermediate second-order thrusts are sometimes discussed (e.g. Teixell et al., 2016, 2018) but are of limited importance for the total amount of shortening as well as for the overall crustal architecture. We sequentially move these thrust structures followed by partial erosion, sedimentation and 6 Myr of thermal re-equilibration. This results in the formation of high relief (using a total shortening of 29 km) together with substantial thickening of the Iberian continental crust from south to north whereas, in contrast, the European continental crust shows a relatively uniform thickness (Figure 6g).

The RIFTER model of the entire collisional evolution of the Western Pyrenees (Figures 6e-g) uses a total of 100 km of shortening including the closing of the former hyper-extended rift basins.

6. Discussion

The purpose of our investigation of the evolution of the Western Pyrenees is to better understand the role of rift structural inheritance during orogeny. We examine both rifting and orogenic histories using structural and stratigraphic modelling that produces cross-sections that are both isostatically as well as structurally balanced.

6.1. Comparison between our model and the target data

Our present-day modelled profile of the Western Pyrenees (Figure 9b) shows a very similar architecture to the target observations (Figures 9a and c).

We are able to reproduce the first-order sub-surface geology of the main domains of the Western Pyrenees across the Mauléon Basin including the Northern (Arzacq) and the Southern Foreland Basins. From north to south these are; the Arzacq Basin, the Northern Mauléon Basin, the Southern Mauléon Basin, the Axial Zone and the Southern Foreland Basin (Figure 9b). However, some parts of our modelled section using RIFTER, such as the Southern Foreland Basin and the Arzacq Basin, require more subsidence to match the target data more precisely. One of the reasons for this misfit may be the value of the effective elastic thickness (Te) used to define the flexural isostatic strength of the lithosphere. The typical Te during continental rifting ranges between 1.5 and 3 km (Roberts et al., 1998; White, 1999; Roberts et al., 2019) while during shortening tectonics this value is usually higher than that. Ford et al., (1992) explored the sensitivity of Te to the lithosphere flexure during thrust sheet emplacement and foreland basin formation and showed that a Te value of 20 km is representative of the foreland region while a lower Te is expected for the centre of the orogen. Jácome et al., (2003) showed that Te = 7.5 km provided the best fit to observations for models of the development of the Maturín Foreland Basin, Eastern Venezuela. In this study we use Te = 1.5 km to calculate the flexural isostatic response for both rifting and contractional tectonics. Not using a higher Te during the contractional history most probably explains the insufficient subsidence predicted for the Arzacq and Southern Foreland Basins (Figure 9b).

Despite this, the Southern and Northern Mauléon Basin as well as the Axial Zone are reasonably well reproduced (Figure 9b) and show the first order stratigraphic architecture as suggested by field observations (Figure 9a). Note that the Southern Mauléon Basin is not well preserved along the eastern Mauléon Basin (Figure 2) and thus we use as reference the outcropping geology ~20 km to the west (Arbailles massif syn-rift syncline, Canérot, 2008) of the target cross-section shown in Figures 4b and 9a to reproduce the Southern Mauléon Basin architecture.

The deeper part of our modelled section shows the southern Iberian Moho at about 30 km depth which gently dips towards the north reaching values of 50 km deep beneath the Mauléon-Arzacq Basin, while the European Moho is more or less horizontal at 20 km deep (Figure 9b). At the larger scale, our modelled deep crustal architecture is similar to that shown by the PYROPE seismic transect of Wang et al., (2016). However, it differs from the seismically imaged Moho beneath the Mauléon Basin (Figure 9c). The PYROPE profile is located across the western part of the Mauléon Basin (Figure 2) where a localized strong positive Bouguer gravity anomaly has been identified (Figure 4e) and interpreted as a piece of exhumed mantle. However, this anomaly is not observed in the eastern Mauléon Basin where the majority of sub-surface geological target observations are obtained (Figure 2). The Moho beneath the Mauléon Basin of our modelled profile is more characteristic of the eastern Mauléon Basin. The overall deep crustal architecture along the Southern Foreland Basin, Axial Zone and Arzacq Basin is expected to be similar across both the eastern and western parts of the Mauléon Basin.

6.2. Uncertainties of deep fault geometry

Fault geometries used to produce our preferred model of the present-day architecture of the Western Pyrenees (Figure 9b) are relatively well constrained for the top 10 to 15 km of depth using surface geology, seismic data and boreholes. However, below these depths, there is little constraint on deep fault geometry. Our preferred model uses deeper fault geometries to give the closest possible agreement to the deep target data (Figure 9c) as well as to the shallower constraints (Figure 9c), however the deeper fault geometries that we have used are not unique. An important question that remains is whether thrust faults within the reactivated necking and proximal rift domains are coupled into the mantle or sole out within the middle-lower crust associated with distributed (pure-shear) deformation below. The evolution of the coupling-depth of faults of other orogenic systems should be investigated to better understand this.

6.3. From rifting to orogeny

Based on the Western Pyrenean example, we suggest a succession of first order tectonic stages that may be used to understand the development of other Alpine type collisional systems. These stages are separated by critical events in geological time that record the change between different tectonic styles of lithosphere deformation. In Figure 10 we show a tectonic evolutionary chart which summarises the deformation mechanism associated with these first order extensional and contractional tectonic stages. The attribution of deformation mechanisms for the rifting stage is based on literature review, while the attribution of deformation mechanisms during the orogenic stage is based on this study.

6.3.1. Rifting evolution

The rifting evolution of the Western Pyrenean example is characterized by three different tectonic phases, each of them respectively bounded by Lower Aptian, Middle Albian and Upper Cenomanian critical events (Figures 10a-c).

During an early rifting stage, the deformation is typically wide and diffuse. This is achieved by faulting in the brittle upper crust soling out at mid-crustal levels (e.g. Stein and Barrientos, 1985, Jackson, 1987) with distributed deformation below in the lower crust and mantle. This typically leads to a slight crustal thinning (e.g. Marsden et al., 1990). In our Western Pyrenees case-study, the first early rifting stage occurred up to the Lower Aptian leading to slight crustal thinning resulting into an overall crustal doming architecture (Figure 10a). In the subsequent necking rift stage, the extensional deformation localizes although it is still achieved by faults decoupled from the mantle which sole out at mid to lower crustal levels (Pérez-Gussinyé et al., 2001; Sutra et al., 2013). During this stage more substantial crustal thinning occurs (Pérez-Gussinyé et al., 2003; Osmundsen and Redfield, 2011, Sutra et al., 2013). This second rifting stage affected the Western Pyrenees up to the Lower Albian. This resulted in high crustal thinning and deepening of the Southern Mauléon and Arzacq Basins (Figure 10b). In our study-case, the necking rifting stage was strongly asymmetric characterized by north-dipping faulting. This is evidenced by: (i) major uplift of the southern flank of the Mauléon Basin (footwall uplift of the lower plate) and (ii) an extension discrepancy between the observed rift structures and the amount of total crustal thinning in the Arzacq Basin. Note that this peculiar asymmetric necking is not always the case and can be more symmetric in other examples (e.g. Lavier and Manatschal, 2006). The third rifting stage consists of hyper-extension rifting where deformation is also localized, however in this case it is achieved by extensional faults coupled into the mantle (Pérez-Gussinyé et al., 2001; Sutra et al., 2013), the maximum penetration depth of which is unknown. In our Western Pyrenean example, this stage lasted up to the Upper Cenomanian critical event leading to the deepening of the Northern Mauléon Basin (Figure 10c).

6.3.2. Pre-orogenic template

In the Western Pyrenees, the post-rifting stage consists of a period of tectonic quiescence characterized by regional thermal subsidence (Figure 10d). This stage, spanning the Upper Cenomanian to Upper Santonian, is bounded by two critical events marking the end of rifting and the onset of orogeny respectively. It is important to point out that the end of this stage (Upper Santonian) corresponds to the pre-orogenic template.

6.3.3. Orogenic evolution

The orogenic evolution of the Western Pyrenees consists of two stages divided by critical events in the Santonian, Eocene and Miocene marking changes in deformation style (Figures 10e-g). The first stage is characterized initially by the reactivation of the hyper-extended domain (i.e. exhumed mantle and hyperthinned domains) followed by the reactivation of the necking domain. This deformation stage, involving the contractional reactivation of hyper-extended and necking rift domains, leads to the recovery of normal crustal thickness (~ 30 km). The second deformation stage is characterized by the shortening of the proximal rift domain consisting of crustal thickening as well as the development of the orogenic root.

Reactivation of hyper-extended domain

According to Péron-Pinvidic et al., (2008) the exhumed continental mantle within the hyper-extended domain corresponds to the weakest part of the margin and thus is a preferred location for the initiation of subduction. This area may become even more weaker if serpentinization of exhumed mantle takes place as suggested by Pérez-Gussinyé et al., (2001) and may consequently generate a weakness within the mantle where the contractional deformation may preferentially initiate (Péron-Pinvidic et al., 2008; Lundin and Doré, 2011; Tugend et al., 2014 and 2015a).

In the Western Pyrenees, the initiation of the reactivation of the hyper-extended domain starts in the Santonian. We show that the deformation during this stage is localized and achieved through extensional fault reactivation within the hyper-extended domain where the Northern Mauléon Detachment system is coupled into the mantle. This reactivated structure pre-configures the continental underthrusting plane and may define, in this case, the vergence of the belt (Figure 10e).

Reactivation of necking domain

How structures developed during the necking rift stage may reactivate during collision is uncertain. One possibility is that the necking-domain extensional faults are reactivated using their original geometry which corresponds to faults soling out within the crust with distributed pure-shear deformation below. However, another possibility is that the reactivated necking-domain extensional faults modify their deeper geometry and couple directly into shallow mantle towards the underthrusting plane. From a geometrical point of view, this would consist of a footwall shortcut that may sample lower crust or even mantle rocks. Whether one fault reactivation mechanism is generally more common than the other is unknown. However, to reproduce the present-day architecture of the Western Pyrenees we use the second hypothesis consisting on the reactivation of the Southern Mauléon Detachment system modifying its deeper geometry and coupling into shallow mantle. This can also explain the occurrence of shallow bodies of mantle rocks that outcrop and/or are suggested from gravity anomalies (Wang et al., 2016).

In any case, the contractional reactivation of the hyper-extended and necking domains results in the closure of the earlier rift basins and leads to the restoration of the thickness of continental crust towards normal values (~30 km) (Figure 10f).

Shortening of proximal domain

Previous geometric or model-based studies such as Teixell et al., (2016) or Jammes et al., (2014) suggested that basement involved thrusts responsible for the collisional stage may be decoupled at about 15 km. Using the Western Pyrenees as an example, we show that to achieve the shortening of the proximal domain, thrusts ramps are decoupled from the mantle by a flat decollement at 25 km depth which laterally branches within the underthrusting plane (ramp). These north-dipping thrusts may be either new faults or reactivated extensional faults (Bellahsen et al., 2012) within the proximal rift domain. As a result of this deformation stage, significant orogenic crustal thickening is produced and hence the Axial Zone is formed (Figure 10g).

The deformation mechanism by which this final stage is achieved differs from that of the earlier convergent stage, involving reactivation of the hyper-extended and necking domains, and thus suggests a critical event between these two stages during the Eocene. The final convergent stage of the Western Pyrenees lasted until the Miocene when contractional deformation ended.

7. Conclusions

Using modelling we investigate the structural and stratigraphic evolution of both the rift and orogenic lithosphere deformation of the Western Pyrenees through a set of isostatically as well as structurally balanced cross-sections. We use this to better understand the role of rift structural inheritance during orogeny.

The key conclusions of this work on the formation of rifted margins and their subsequent development into orogens are the following:

1- The present-day structure of the Western Pyrenees orogen has been reproduced by including the extensional as well as the compressional history of lithosphere deformation.
2- The earlier extensional tectonic of the Western Pyrenees is characterized by a Cretaceous hyper-extended rift system. This is followed by contractional tectonics consisting of two sequential deformation stages: (i) the reactivation of the hyper-extended and necking rift domains and (ii) the shortening of the proximal rift domain.
3- Using the Western Pyrenees as an example, we suggest the following insights on the deeper fault geometries during orogeny, although this still needs to be compared with other orogenic systems. The contractional reactivation of the

hyper-extended rift domain uses faults which are coupled into the mantle. The contractional reactivation of the necking rift domain uses faults which modify their deeper geometry and couple into shallow mantle. The shortening of the proximal rift domain on the pro-side of the belt is achieved by thrusts ramps which laterally link into the continental underthrusting ramp plane.

We believe that the tectonic evolutionary chart derived from this study, which summarises the extensional and contractional lithosphere deformation stages, may be applied to other Alpine-type collisional systems involving the reactivation and inversion of former hyper-extended rift domains.

Acknowledgments

We acknowledge the MM4 (Margin Modelling Phase 4) industry partners (BP, Conoco Phillips, Statoil, Petrobras, Total, Shell, BHP-Billiton, and BG) for financial support and discussions. We thank Total SA and notably S. Calassou for allowing the use of seismic and well data across the Arzacq Basin and publication of proprietary seismic line nº1325. E.M. acknowledge the Orogen research program for fruitful discussions. J.G-R. thanks A. Lamur for collaborate in the development of a new MATLAB code used to display the graphics of all RIFTER models presented here. The original manuscript was improved by reviews from S. Tavani, an anonymous reviewer and by guest editors O. Lacombe and S. Mazzoli, who we thank for their helpful comments.

REFERENCES

Andersen, T.B., Corfu, F., Labrousse, L., Osmundsen, P.-T., 2012. Evidence for hyperextension along the pre-Caledonian margin of Baltica. J. Geol. Soc. London. 169, 601–612. https://doi.org/10.1144/0016-76492012-011.

Angrand, P., Ford, M., & Watts, A. B. (2018). Lateral variations in foreland flexure of a rifted continental margin: The Aquitaine Basin (SW France). Tectonics, 37(2), 430-449.

Bellahsen, N., Jolivet, L., Lacombe, O., Bellanger, M., Boutoux, A., Garcia, S., Mouthereau, F., Le Pourhiet, L., Gumiaux, C., 2012. Mechanisms of margin inversion in the external Western Alps: Implications for crustal rheology. Tectonophysics 560–561, 62–83. https://doi.org/10.1016/j.tecto.2012.06.022.

Beltrando, M., Manatschal, G., Mohn, G., Dal Piaz, G.V., Vitale Brovarone, A., Masini, E., 2014. Recognizing remnants of magma-poor rifted margins in high-pressure orogenic belts: The Alpine case study. Earth-Science Rev. 131, 88–115. doi:10.1016/j.earscirev.2014.01.001.

Biteau, J.-J., Le Marrec, A., Le Vot, M., Masset, J.-M., 2006. The Aquitaine Basin. Pet. Geosci. 12, 247–273. doi:10.1144/1354-079305-674.

Bosch, G. V., Teixell, A., Jolivet, M., Labaume, P., Stockli, D., Domènech, M., Monié, P., 2016. Timing of Eocene-Miocene thrust activity in the Western Axial Zone and Chaînons Béarnais (west-central Pyrenees) revealed by multi-method thermochronology. Comptes Rendus - Geosci. 348, 246–256. https://doi.org/10.1016/j.crte.2016.01.001.

Brgm, Esso, S., 1974. Géologie du bassin d'Aquitaine. Orléans, France.

Brunet, M.F., 1984. Subsidence history of the Aquitaine basin determined from subsidence curves. Geol. Mag. 121, 421–428. doi:10.1017/S0016756800029952.

Burg, J.-P., 1994. Syn-to post-thickening extension in the Variscan Belt of Western Europe: modes and structural consequences. Géologie la Fr. 3, 33–51.

Canérot, J., 2008. Les Pyrénées: histoire géologique et itinéraires de découverte. Biarrtiz: Atlantica/BRGM éds., 2, 646 p.

Canérot, J., Majeste-Menjoulas, C., Ternet, Y., James, V., Fabre, R., Desrumaux, C., Lebourg, T., 2001. Les glissements rocheux du versant sud du Layens (Vallée d'Aspe, Pyrénées occidentales). Bull. la Société géologique Fr. 172, 779–784.

Canérot, J., 1989. Early Cretaceous rifting and salt tectonics on the Iberian margin of the western Pyrenees (France). Structural consequences. Bull. Tech. Explor. Elf Aquitaine 13 (1), 87–99.

Capote, R., Muñoz, J.A., Simón, J., 2002. Alpine tectonics. I: The Alpine system north of the Betic Cordillera. Geol. Soc. London, Spec. Publ. n W. Gibbo, 367–400.

Casas, A., Kearey, P., Rivero, L., Adam, C., 1997. Gravity anomaly map of the Pyrenean region and a comparison of the deep geological structure of the western and eastern Pyrenees. Earth Planet. Sci. Lett. 150, 65–78. doi:10.1016/S0012-821X(97)00087-3.

Casteras, M., 1969. Geological map sheet of Mauléon-Licharre, 1/80000. BRGM Orléans, France.

Chevrot, S., Sylvander, M., Diaz, J., Ruiz, M., Paul, A., Cougoulat, G., Péquegnat, C., Wolyniec, D., Delmas, P., Grimaud, F., Benahmed, S., Pauchet, H., de Saint Blanquat, M., Lagabrielle, Y., Manatschal, G., 2015. The Pyrenean architecture as revealed by teleseismic P-to-S converted waves recorded along two dense transects. Geophys. J. Int. 200, 1096–1107. doi:10.1093/gji/ggu400.

Chevrot, S., Sylvander, M., Diaz, J., Martin, R., Mouthereau, F., Manatschal, G., Masini, E., Calassou, S., Grimaud, F., Pauchet, H., Ruiz, M., 2018. The non-cylindrical crustal architecture of the Pyrenees 1–8. https://doi.org/10.1038/s41598-018-27889-x.

Choukroune, P., Pinet, B., Roure, F., Cazes, M., 1990. Major Hercynian thrusts along the ECORS Pyrenees and Biscay lines. Bull. la Société géologique Fr. 2, 313–320.

Clerc, C., Lagabrielle, Y., Neumaier, M., Reynaud, J.-Y., de Saint Blanquat, M., 2012. Exhumation of subcontinental mantle rocks: evidence from ultramafic-bearing clastic deposits nearby the Lherz peridotite body, French Pyrenees. Bull. la Soc. Geol. Fr. 183, 443–459. https://doi.org/10.2113/gssgfbull.183.5.443.

Clerc, C., Lagabrielle, Y., 2014. Thermal control on the modes of crustal thinning leading to mantle exhumation: Insights from the cretaceous pyrenean hot paleomargins. Tectonics 33. https://doi.org/10.1002/2013TC003471.

Cochelin, B., Lemirre, B., Denèle, Y., de Saint Blanquat, M., Lahfid, A., & Duchêne, S. (2018). Structural inheritance in the Central Pyrenees: the Variscan to Alpine tectonometamorphic evolution of the Axial Zone. Journal of the Geological Society, 175(2), 336-351.

Daignières, M., Séguret, M., Specht, M., ECORS, T., 1994. The Arzacq-Western Pyrenees ECORS deep seismic profile. Publ. Eur. Assoc. Pet. Geol. 4, 199–208.

Dumont, T., Replumaz, A., Rouméjon, S., Briais, A., Rigo, A., Bouillin, J.P., 2015. Microseismicity of the Béarn range: Reactivation of inversion and collision structures at the northern edge of the Iberian plate. Tectonics, 34, doi:10.1002/2014TC003816.

Epin, M., 2017. Defining diagnostic criteria to describe the role of rift inheritance in collisional orogens : the case of the Err-Platta nappes (Switzerland). Swiss J Geosci, doi:10.1007/s00015-017-0271-6.

Ford, M., Lickorish, W.H., Kusznir, N.J., 1999. Tertiary foreland sedimentation in the Southern Subalpine Chains, SE France: A geodynamic appraisal. Basin Res. 11, 315–336. doi:10.1046/j.1365-2117.1999.00103.

Gallastegui, J., Pulgar, J.A., Gallart, J., 2002. Initiation of an active margin at the North Iberian continent-ocean transition. Tectonics 21, 1–14. doi:10.1029/2001TC901046.

Garrido-Megías, A., Ríos, L., 1972. Síntesis geologica del Secundario y Terciario entre los ríos Cinca y Segre (Pirineo Central de la vertiente surpirenaica, provincias de Huesca y Lerida). Bol. Geol. Min 83, 1–47.

Grandjean, G., 1994. Etude des structures crustales dans une portion de chaîne et de leur relation avec les bassins sédimentaires. Application aux Pyrenees occidentales. Bull. la Société géologique Fr. Explor. Elf-Aquitaine Prod 18, 391–419.

Grool, A.R., Ford, M., Vergés, J., Huismans, R.S., Christophoul, F., Dielforder, A., 2018. Insights Into the Crustal-Scale Dynamics of a Doubly Vergent Orogen From a Quantitative Analysis of Its Forelands: A Case Study of the Eastern Pyrenees. Tectonics 37, 450–476. https://doi.org/10.1002/2017TC004731.

Jackson, J., 1987. Active normal faulting and crustal extension. Geol. Soc. London, Spec. Publ. 28, 3–17. doi:10.1144/GSL.SP.1987.028.01.02.

Jácome, M.I., Kusznir, N., Audemard, F., Flint, S., 2003. Formation of the Maturín Foreland Basin, eastern Venezuela: Thrust sheet loading or subduction dynamic topography. Tectonics 22, n/a-n/a. https://doi.org/10.1029/2002tc001381.

James, V., Canérot, J., Biteau, J. J., 1996. Données nouvelles sur la phase de rifting atlantique des Pyrénées occidentales au Kimméridgien: La masse glissée d'Ouzous (Hautes Pyrénées), Géol. France 3, 60–66.

James, V., Canérot, J., 1999 Diapirisme et structuration post-triasique des Pyrénées occidentales et de l'aquitaine méridionales (France). Eclogae Geol Helv 92:63–

72.

Jammes, S., Manatschal, G., Lavier, L., Masini, E., 2009. Tectonosedimentary evolution related to extreme crustal thinning ahead of a propagating ocean: Example of the western Pyrenees. Tectonics, 28, TC4012, doi:10.1029/2008TC002406.

Jammes, S., Lavier, L., Manatschal, G., 2010a. Extreme crustal thinning in the Bay of Biscay and the Western Pyrenees: From observations to modeling. Geochem. Geophys. Geosyst., 11, Q10016, doi:10.1029/2010GC003218.

Jammes, S., Manatschal, G., Lavier, L., 2010b. Interaction between prerift salt and detachment faulting in hyperextended rift systems : The example of the Parentis and Mauléon basins (Bay of Biscay and western Pyrenees). AAPG Bulletin, v. 94, num 7, 957–975. doi:10.1306/12090909116.

Jammes, S., Huismans, R.S., Muñoz, J.A., 2014. Lateral variation in structural style of mountain building: Controls of rheological and rift inheritance. Terra Nova, 26, 201–207. doi:10.1111/ter.12087.

Jourdon, A., Le Pourhiet, L., Mouthereau, F., Masini, E., 2019. Role of rift maturity on the architecture and shortening distribution in mountain belts. Earth Planet. Sci. Lett. 512, 89–99. https://doi.org/S0012821X19300937.

Lacombe, O., Bellahsen, N., 2016. Thick-skinned tectonics and basement-involved fold-thrust belts: Insights from selected Cenozoic orogens, Geological Magazine. https://doi.org/10.1017/S0016756816000078.

Lagabrielle, Y., Bodinier, J., 2008. Submarine reworking of exhumed subcontinental mantle rocks : field evidence from the Lherz peridotites. French Pyrenees 11–21. doi:10.1111/j.1365-3121.2007.00781.

Lagabrielle, Y., Labaume, P., Blanquat, M.D. Saint, 2010. Mantle exhumation , crustal denudation , and gravity tectonics during Cretaceous rifting in the Pyrenean realm (SW Europe): Insights from the geological setting of the lherzolite bodies. Tectonics, 29, TC4012, doi:10.1029/2009TC002588.

Lavier, L., Manatschal, G., 2006. Mechanism to thin continental lithosphere at magma poor margins. Nature 440:324-328.

Lemoine, M., Tricart, P., Boillot, G., 1987. Ultramafic and gabbroic ocean floor of the Ligurian Tethys (Alps, Corsica, Apennines): in search of a genetic model. Geology 15, 622–625. https://doi.org/10.1130/0091-7613.

Le Pichon, X., Sibuet, J.-C., 1971. Western extension of boundary between European and Iberians plates during the Pyrenean orogeny. Earth Planet. Sci. Lett. 12, 83–88.

Le Pochat, G., Lenguin, M., Thibault, C., 1976. Carte géologique de la France à 1/50 000, feuille nº XIV-45, Mauléon-Licharre, avec notice explicative. Orléans: BRGM éd, 24 p.

Le Pochat, G., Lenguin, M., Napias, J.-C., Thibaut, C., Roger, P., Bois, J.-P., 1978. Carte géologique de la France à 1/50 000, feuille nº XIII-46, Saint-Jean-Pied-de-Port, avec notice explicative. Orléans: BRGM éd, 41.

Lundin, E.R., Doré, A.G., 2011. Hyperextension, serpentinization, and weakening: A new paradigm for rifted margin compressional deformation. Geology 39, 347–350. doi:10.1130/G31499.1.

Macchiavelli, C., Vergés, J., Schettino, A., Fernàndez, M., Turco, E., Casciello, E., Tunini, L. (2017). A new southern North Atlantic isochron map: Insights into the drift of the Iberian plate since the Late Cretaceous. Journal of Geophysical Research: Solid Earth, 122(12), 9603-9626.

Manatschal, G., 2004. New models for evolution of magma-poor rifted margins based on a review of data and concepts from West Iberia and the Alps. Int. J. Earth Sci. 93, 432–466. https://doi.org/10.1007/s00531-004-0394-7.

Masini, E., Manatschal, G., Mohn, G., Unternehr, P., 2012. Anatomy and tectono-sedimentary evolution of a rift-related detachment system : The example of the Err detachment (central Alps, SE Switzerland). GSA Bull. 1535–1551. https://doi.org/10.1130/B30557.1.

Masini, E., Manatschal, G., Tugend, J., Mohn, G., Flament, J.M., 2014. The tectono-sedimentary evolution of a hyper-extended rift basin: The example of the Arzacq-Maul??on rift system (Western Pyrenees, SW France). Int. J. Earth Sci. 103, 1569–1596. doi:10.1007/s00531-014-1023-8.

Marsden, G., Yielding, G., Roberts, A., Kusznir, N., 1990. Application of a flexural cantilever simple-shear/pure-shear model of continental lithosphere extension to the formation of the northern North Sea basin. In: D.J. Blundell and A.D. Gibbs (Editors), Tectonic Evolution of the North Sea Rifts. Oxford Univ, Press 236–257.

Mattauer, M., Henry, J., 1974. The Pyrenees, in Mesozoic-Cenozoic Orogenic Belts. Data for orogenic Studies: Alpine-Himalayan Orogens, edited by A. M. Spencer. Geol. Soc. London Spec. Publ 4,3-21.

McClay, K., Muñoz, J.A., García-Senz, J., 2004. Extensional salt tectonics in a contractional orogen : A newly identified tectonic event in the Spanish Pyrenees. Geology, v.4, 737–740. https://doi.org/10.1130/G20565.1.

Mohn, G., Manatschal, G., Müntener, O., Beltrando, M., Masini, E., 2010. Unravelling the interaction between tectonic and sedimentary processes during lithospheric thinning in the Alpine Tethys margins. Int. J. Earth Sci. 99, 75–101. https://doi.org/10.1007/s00531-010-0566-6.

Mohn, G., Manatschal, G., Beltrando, M., Haupert, I., 2014. The role of rift-inherited hyper-extension in Alpine-type orogens. Terra Nov. 26, 347–353. https://doi.org/10.1111/ter.12104.

Montadert, L., Roberts, D.G., 1979. Initial Reports of the Deep Sea Drilling Project, 48 pp., US Governmment Printing Office, Washington, D.C.

Montadert, L., De Charpal, O., Roberts, D., Guennoc, P., Sibuet, J.-C., 1979. Northeast Atlantic passive continental margins: Rifting and subsidence processes. In: Talwani, M., Hay, W. & Ryan, W. B. F. (eds) Deep Drilling Results in the Atlantic Ocean: Continental Margins and Palaeoenvironments. Am. Geophiscal Union, Washington, DC 154–186.

Mouthereau, F., Filleaudeau, P.-Y., Vacherat, A., Pik, R., Lacombe, O., Guiditta-Fellin, M., Castelltort, S., Christophoul, F., Masini, E., 2014. Placing limits to shortening evolution in the Pyrenees: Role of margin architecture and implications for the Iberia/Europe convergence. Tectonics, 33, doi:10.1002/2014TC003663.

Muñoz, J.A., 2002. The Pyrenees. Gibbons W., Moreno, T. 370–385.

Muñoz, J.A., 1992. Evolution of a continental collision belt: ECORS-Pyrenees crustal balanced section, in Thrust Tectonics edited by K.R. McClay 235–246.

Nirrengarten, M., Manatschal, G., Tugend, J., Kusznir, N., Sauter, D., 2018. Kinematic Evolution of the Southern North Atlantic: Implications for the Formation of Hyperextended Rift Systems. Tectonics, 37, 89–118.doi:10.1002/2017TC004495.

Olivet, J.L., 1996. La cinématique de la plaque Ibérique. Bull. Cent. Rech. Explor. Prod. Elf Aquitaine 20, 131–195.

Osmundsen, P.T., Redfield, T.F., 2011. Crustal taper and topography at passive continental margins. Terra Nova, 23, 349-361. doi:10.1111/j.1365-3121.2011.01014.

Pedreira, D., Pulgar, J.A., Gallart, J., Torné, M., 2007. Three-dimensional gravity and magnetic modeling of crustal indentation and wedging in the western Pyrenees-Cantabrian Mountains. J. Geophys. Res. Solid Earth 112, 1–19. doi:10.1029/2007JB005021.

Pérez-Gussinyé, M., Ranero, C., Reston, T., Sawyer, D., 2003. Mechanisms of extension at nonvolcanic margins: Evidence from the Galicia interior basin, west of Iberia. J. Geophys. Res. 108, 1–19. doi:10.1029/2001JB000901.

Pérez-Gussinyé, M., Reston, T.J., Phipps Morgan, J., 2001. Serpentinization and magmatism during extension at non-volcanic margins: the effect of initial lithospheric structure. Geol. Soc. London, Spec. Publ. 187, 551–576. doi:10.1144/GSL.SP.2001.187.01.27.

Péron-Pinvidic, G., Manatschal, G., Dean, S.M., Minshull, T.A., 2008. Compressional structures on the West Iberia rifted margin: Controls on their distribution, in Johnson, H., et al., eds., The nature and origin of compression in passive margins. Geol. Soc. London, Spec. Publ. 306, 169–183. doi:10.1144/SP306.8.

Pulgar, J.A., Gallart, J., Fernandez-Viejo, G., Perez-Estaun, A., Alvarez-Marron, J., Alonso, J.L., Gallastegui, J., Marcos, A., Bastida, F., Aller, J., Farias, P., Marín, J., García-Espina, R., Martínez-Catalán, J.R., Comas, M.C., Banda, E., Dańobeitia, J.J., Córdoba, D., Heredia, N., Rodríguez, R., 1996. Seismic image of the Cantabrian Mountains in the western extension of the Pyrenees from integrated ESCIN reflection and refraction data. Tectonophysics 264, 1–19.

https://doi.org/10.1016/S0040-1951(96)00114-X.

Rat, J., Mouthereau, F., Brichau, S., Crémades, A., Bernet, M., Balvay, M., Ganne, J., Lahfid, A., Gautheron, C., 2019. Tectonothermal Evolution of the Cameros Basin: Implications for Tectonics of North Iberia. Tectonics. https://doi.org/10.1029/2018TC005294.

Roberts, A.M., Kusznir, N.J., Yielding, G., Styles, P., 1998. 2D flexural backstripping of extensional basins; the need for a sideways glance. Pet. Geosci. 4, 327–338. https://doi.org/10.1144/petgeo.4.4.327.

Roberts, A.M., Kusznir, N.J., Yielding, G., Beeley, H., 2019. Mapping the bathymetric evolution of the northern North Sea: from Jurassic syn-rift archipelago through Cretaceous-Tertiary post-rift subsidence. Pet. Geosci.

Roca, E., Muñoz, J.A., Ferrer, O., Ellouz, N., 2011. The role of the Bay of Biscay Mesozoic extensional structure in the configuration of the Pyrenean orogen: Constraints from the MARCONI deep seismic reflection survey. Tectonics, 30, 1–33. doi:10.1029/2010TC002735.

Rocher, M., Lacombe, O., Angelier, J., Deffontaines, B., Verdier, F., 2000. Cenozoic folding and faulting in the south Aquitaine Basin (France): Insights from combined structural and paleostress analyses. J. Struct. Geol. 22, 627–645. https://doi.org/10.1016/S0191-8141(99)00181-9.

Roest, W.R., Srivastava, S.P., 1991. Kinematics of the plate boundaries between Eurasia, Iberia, and Africa in the North Atlantic from the Late Cretaceous to the present. Geology, 19, 613–616. doi:10.1130/0091-7613.

Rosenbaum, G., Lister, G.S., Duboz, C., 2002. Relative motions of Africa, Iberia and Europe during Alpine orogeny. Tectonophysics 359, 117–129. doi:10.1016/S0040-1951(02)00442-0.

Roure, F., Choukroune, P., Mu, J.A., Camara, P., Researcher, I., Iberian, S.W., Tethys, L., 1989. ECORS Deep seismic data and balanced cross- section ; geometric constraints on the evolution of the Pyrenees. Tectonics, vol 8, num 1. doi:10.1029/TC008i001p00041.

Salas, R., Casas, A., 1993. Mesozoic extensional tectonics, stratigraphy and crustal evolution during the Alpine cycle of the eastern Iberian basin. Tectonophysics 228, 33–55. doi:10.1016/0040-1951(93)90213-4.

Saspiturry, N., Razin, P., Baudin, T., Serrano, O., Issautier, B., Lasseur, E., Allanic, C., Thinon, I., Leleu, S., 2019. Symmetry vs. asymmetry of a hyper-thinned rift: Example of the Mauléon Basin (Western Pyrenees, France). Mar. Pet. Geol. 104, 86–105. https://doi.org/10.1016/j.marpetgeo.2019.03.031.

Schettino, A., Scotese, C.R., 2002. Global kinematic constraints to the tectonic history of the Mediterranean region and surrounding areas during the Jurassic and cretaceous. J. Virtual Explor. 8. doi:10.3809/jvirtex.2002.00056.

Serrano, O., Delmas, J., Hanot, F., Vially, R., Herbin, J.P., Houel, P., Tourlière, B., 2006. Le bassin d'Aquitaine: Valorisation des données sismiques, cartographie structurale et potentiel pétrolier. Rapp. Régional d'Evaluation Pétrolière. Bur. la Rech. Géologique Minière, Orléans, Fr. 245.

Sibuet, J.-C., Collette, B.J., 1991. Triple junctions of Bay of Biscay and North Atlantic: New constraints on the kinematic evolution. Geol. 19E. Banda, 525.

Srivastava, S.P., Roest, W.R., Kovacs, L.C., Oakey, G., Lévesque, S., Verhoef, J., Macnab, R., 1990. Motion of Iberia since the Late Jurassic: Results from detailed aeromagnetic measurements in the Newfoundland Basin. Tectonophysics 184, 229–260. doi:10.1016/0040-1951(90)90442-B.

Stein, R.-S., Barrientos, S.-E., 1985. Planar High-Angle Faulting in the Basin and Range: Geodetic Analysis of the 1983 Borah Peak, Idaho, Earthquake. J. Geophys. Res. 90, 11,355-11,366.

Sutra, E., Manatschal, G., Mohn, G., Unternehr, P., 2013. Quantification and restoration of extensional deformation along the Western Iberia and Newfoundland rifted margins. Geochemistry, Geophys. Geosystems 14, 2575–2597. doi:10.1002/ggge.20135.

Tavani, S., Bertok, C., Granado, P., Piana, F., Salas, R., Vigna, B., Muñoz, J.A., 2018. The Iberia-Eurasia plate boundary east of the Pyrenees. Earth-Science Rev. 187, 314–337. https://doi.org/10.1016/j.earscirev.2018.10.008.

Teixell, A., 1998. Crustal structure and orogenic material budget in the west central

Pyrenees. Tectonics, vol 17, num 3, 395–406.

Teixell, A., 1990. Alpine thrusts at the western termination of the Pyrenean Axial Zone. Bull. la Société géologique Fr. 8(6), 241–249.

Teixell, A., Labaume, P., Lagabrielle, Y., 2016. The crustal evolution of the west-central Pyrenees revisited: Inferences from a new kinematic scenario. Comptes Rendus - Geosci. 348, 257–267. doi:10.1016/j.crte.2015.10.010.

Teixell, A., Labaume, P., Ayarza, P., Espurt, N., de Saint Blanquat, M., Lagabrielle, Y., 2018. Crustal structure and evolution of the Pyrenean-Cantabrian belt: A review and new interpretations from recent concepts and data. Tectonophysics 724–725, 146–170. https://doi.org/10.1016/j.tecto.2018.01.009.

Toth, J., Kusznir, N.J., Flint, S.S., 1996. A flexural isostatic model of lithosphere shortening and foreland basin formation: Application to the Eastern Cordillera and Subandean belt of NW Argentina. Tectonics 15, 2–3.

Tugend, J., Manatschal, G., Kusznir, N.J., 2015a. Spatial and temporal evolution of hyperextended rift systems: Implication for the nature, kinematics, and timing of the Iberian- European plate boundary. Geology, 15–18. doi:10.1130/G36072.1.

Tugend, J., Manatschal, G., Kusznir, N.J., Masini, E., 2015b. Characterizing and identifying structural domains at rifted continental margins: application to the Bay of Biscay margins and its Western Pyrenean fossil remnants. Geological Society, London, Special Publications, 413.10.1144/SP413.3.

Tugend, J., Manatschal, G., Kusznir, N.J., Masini, E., Mohn, G., Thinon, I., 2014. Formation and deformation of hyperextended rift systems: Insights from rift domain mapping in the Bay of Biscay-Pyrenees, Tectonics, 33, 1239-1276, doi:10.1002/2014TC003529.

Vacher, P., Souriau, A., 2001. A three-dimensional model of the Pyrenean deep structure based on gravity modelling, seismic images and petrological constraints. Geophys. J. Int. 145, 460–470.

Vacherat, A., Mouthereau, F., Pik, R., Huyghe, D., Paquette, J.L., Christophoul, F., Loget, N., Tibari, B., 2017. Rift-to-collision sediment routing in the Pyrenees: A synthesis from sedimentological, geochronological and kinematic constraints.

Earth-Science Rev. 172, 43–74. https://doi.org/10.1016/j.earscirev.2017.07.004.

Vergés, J., Millán, H., Roca, E., Muñoz, J.A., Marzo, M., Cirés, J., Bezemer, T. Den, Zoetemeijer, R., Cloetingh, S., 1995. Eastern Pyrenees and related foreland basins: pre-, syn- and post-collisional crustal-scale cross-sections. Mar. Pet. Geol. 12, 903–915. https://doi.org/10.1016/0264-8172(95)98854-X.

Vergés, J., Fernàndez, M., Martìnez, A., 2002. The Pyrenean orogen: Pre-, syn-, and post-collisional evolution. J. Virtual Explor. 8. doi:10.3809/jvirtex.2002.00058.

Vergés, J., García-Senz, J., 2001. Mesozoic evolution and Cainozoic inversion of the Pyrenean rift. Peri-Tethys Mem. 6 Peri-Tethyan Rift. Mém. Mus. natn. Hist, nat. 186, 187–212.

Wang, Y., Chevrot, S., Monteiller, V., Komatitsch, D., Mouthereau, F., Manatschal, G., Sylvander, M., Diaz, J., Ruiz, M., Grimaud, F., Benahmed, S., Pauchet, H., Martin, R., 2016. The deep roots of the western Pyrenees revealed by full waveform inversion of teleseismic P waves. Geology 44. doi:10.1130/G37812.1.

White, R.S., 1999. The lithosphere under stress. Philos. Trans. R. Soc. A Math. Phys. Eng. Sci. 357, 901–915. https://doi.org/10.1098/rsta.1999.0357.

Wilson, J., 1966. Did the atlantic close and then reopen?. Nature 211, 286. doi:10.12789/geocanj.2016.43.109.

Singe column width **Figure 1**

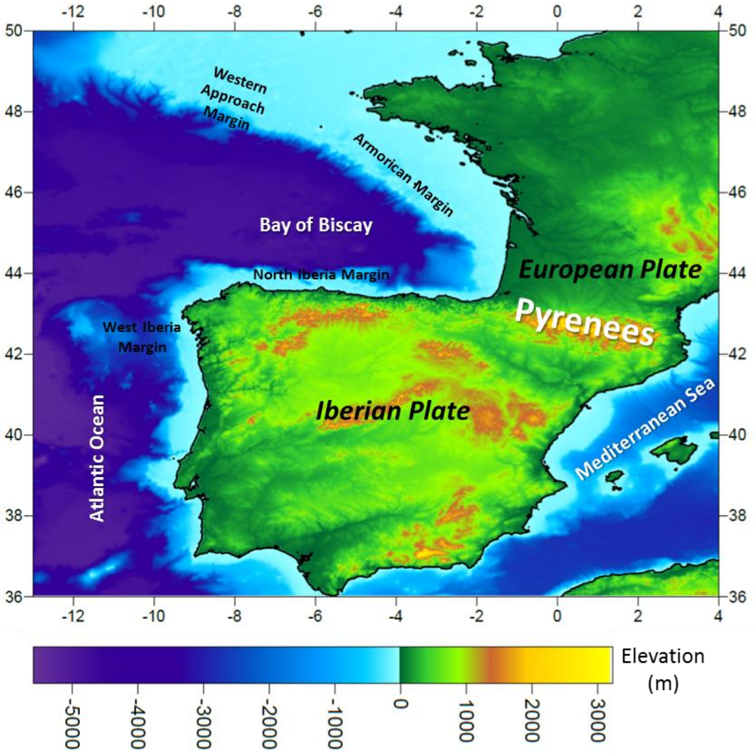

Figure 1: Bathymetric and topographic map of the Iberian and European plates, showing the location of the Bay of Biscay and Pyrenees.

Double column width **Figure 2**

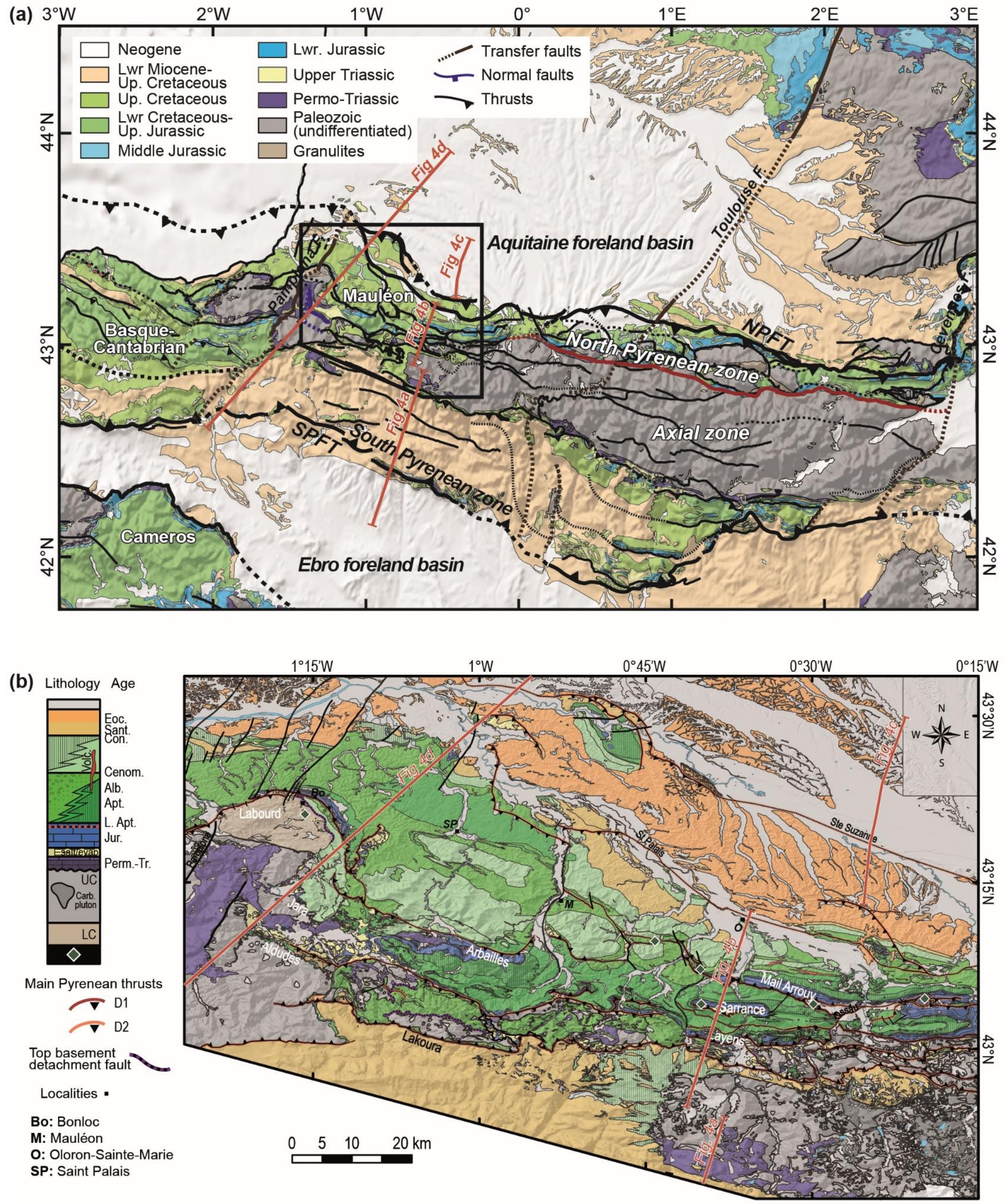

Figure 2: a) Geological map of the Western Pyrenean orogen. The black polygon shows the position of the Mauléon Basin map shown in **b).** This map is modified after the BRGM 1 million map. **b)** Geological map of the Mauléon basin as shown in Tugend et al., (2014 and 2015). Lithologies and age of sequences are synthetized in a log. The red lines indicate the location of the geological sections shown in Figures 4a-c and the position of the PYROPE seismic transect (Chevrot et al., 2015) shown in Figure 4d.

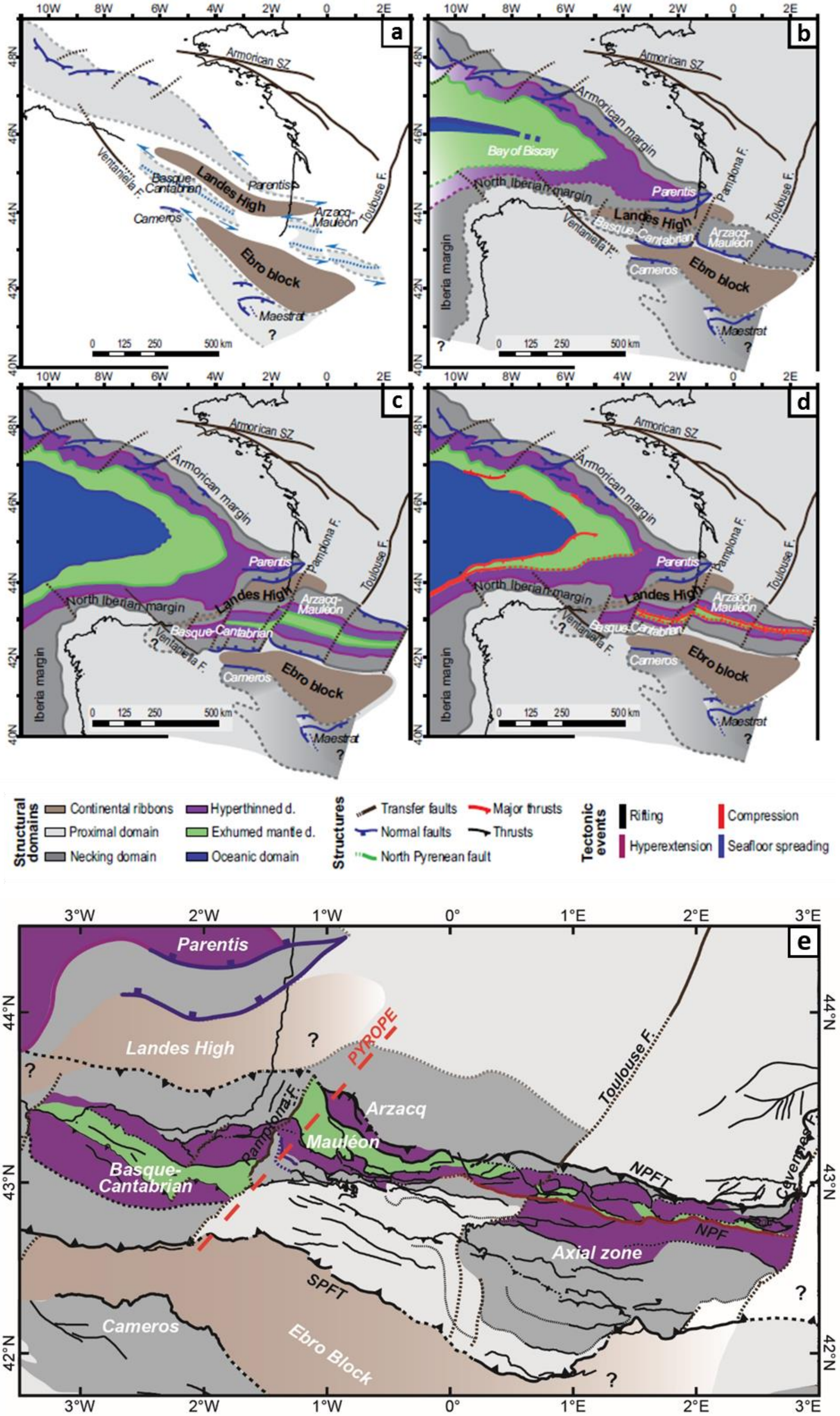

Figure 3: a), b), c) and **d)** Restoration showing the spatial and temporal evolution of the Iberian-European plate boundary from Tugend et al., (2015). **a)** Initiation of transtensional rifting stage (Late Jurassic). **b)** Sea-floor spreading initiation and northeast-southwest extension (Aptian-Albian). **c)** Failed tentative localization of plate boundary (before Santonian). **d)** Subduction initiation (Late Cretaceous). **e)** Rift domains map of the Pyrenean-Cantabrian rift system (after Tugend et al., 2014). The red dashed line shows the position of the PYROPE seismic transect (Chevrot et al., 2015) shown in Figure 4d.

Double column width

Figure 4

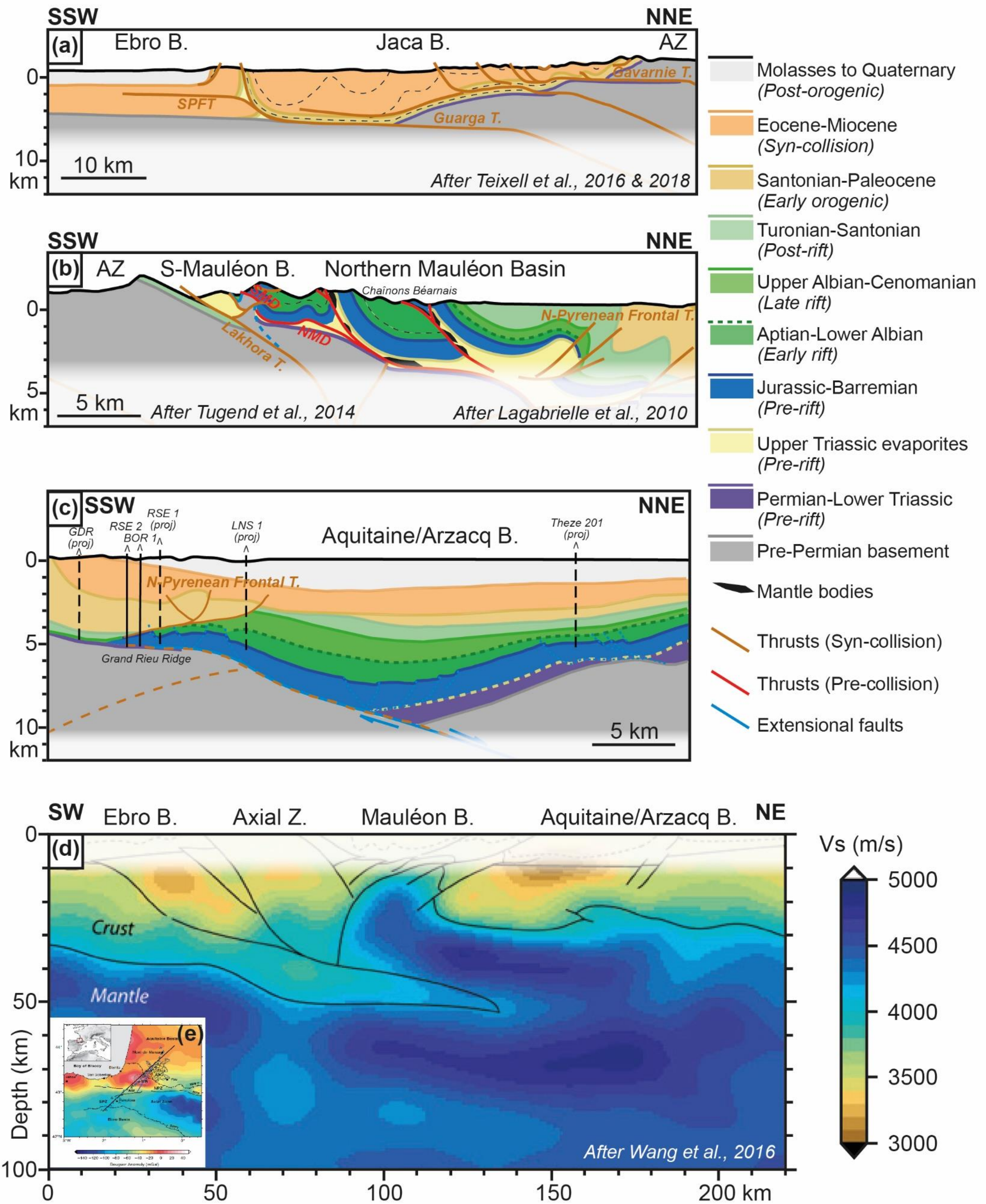

Figure 4: a), b) and **c)** Present-day geological cross-sections across the Western Pyrenees. **a)** and **b)** Are constrained using published cross-sections and mainly based on field observations while **c)** is constrained using seismic line nº1325 and well logs (black lines) owned by Total SA (seismic line is shown in Appendix 1). **d)** Vs seismic velocity model obtained by full waveform inversion and its interpretation along the PYROPE seismic transect located in the Western Pyrenees (Wang et al., 2016). **e)** Map of Bouguer gravity anomaly with the location of the seismic stations (blue triangles) as well as the location of the PYROPE transect (black line) (Wang et al., 2016). **AZ:** Axial Zone, **S-Mauléon B.:** Southern Mauléon Basin, **SPFT:** South Pyrenean Frontal Thrust, **SMD:** Southern Mauléon Detachment, **NMD:** Northern Mauléon Detachment; **N-Pyrenean Frontal T.:** North Pyrenean Frontal Thrust.

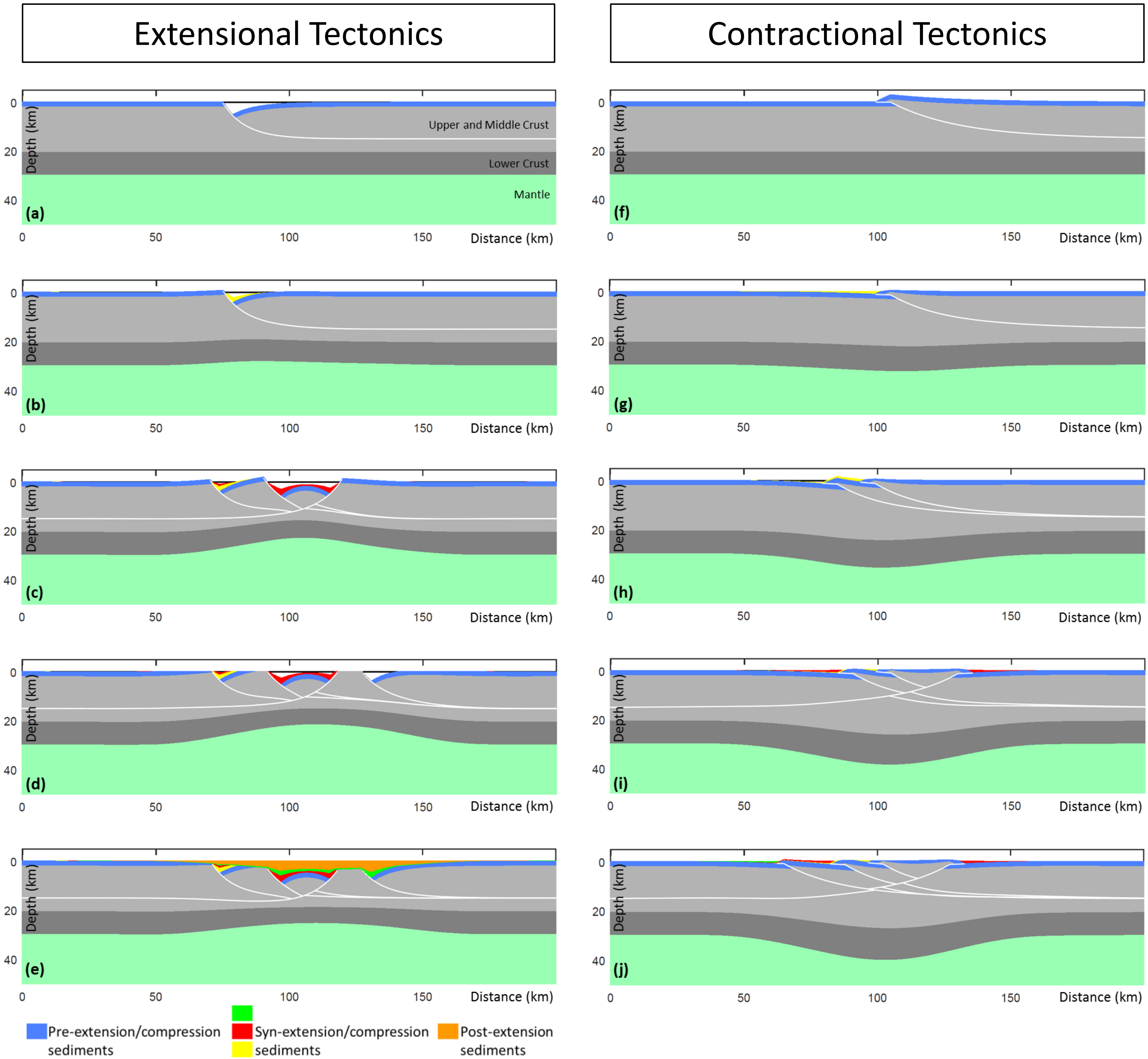

Figure 5: The RIFTER model applied to extensional (**a-e**) and contractional (**f-j**) tectonics. **a)** and **f)** show faulting alone with no deep pure-shear deformation below. **b-e)** and **g-j)** show the lithosphere response to sequential faulting, deeper lithosphere deformation giving crustal thinning or thickening, sediment loading, erosional unloading, lithosphere thermal perturbation and re-equilibration and their flexural isostatic responses. See text for more explanation**.**

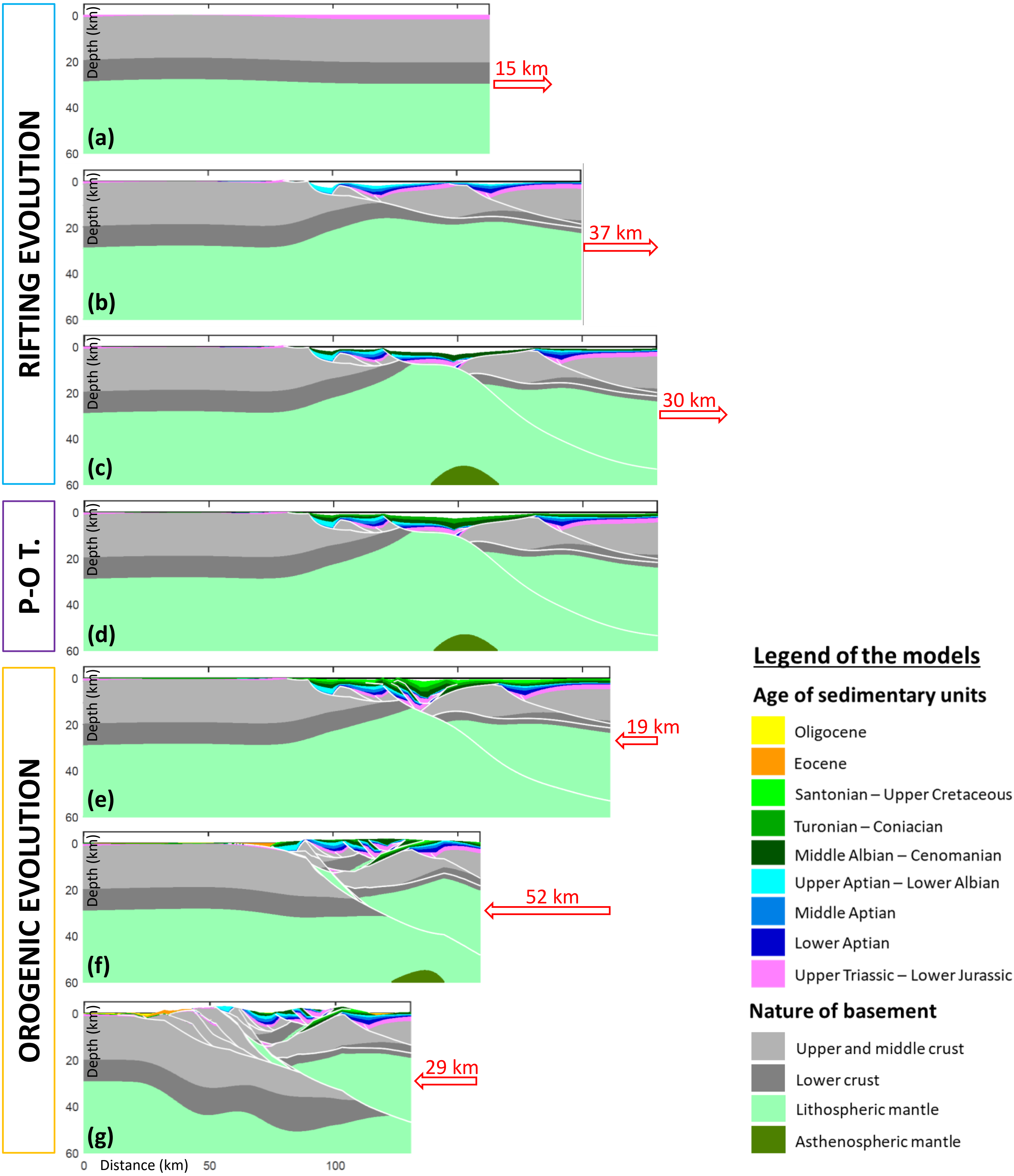

Figure 6: Rifting and orogenic evolution of the Western Pyrenees using a kinematic structural-stratigraphic forward model (RIFTER). The rifting evolution is shown in **a-c)**, the pre-orogenic template obtained at the end of rifting and used to start the orogenic evolution is show in **d)**, and the orogenic evolution is shown in **e-g)**. **a)** Early rifting with lithosphere extended by 15 km. **b)** Necking rifting with lithosphere extended by 37 km. **c)** Hyper-extension rifting with lithosphere extended by 30 km. **d)** Post-rifting giving the pre-orogenic template (**P-O T**.). **e)** Reactivation of hyper-extended domain with lithosphere shortened by 19 km. **f)** Reactivation of necking domain with lithosphere shortened by 52 km. **g)** Shortening of proximal domain with lithosphere shortened by 29 km. Age of sedimentary units and the nature of the basement are shown in the legend.

Double column width

Figure 7

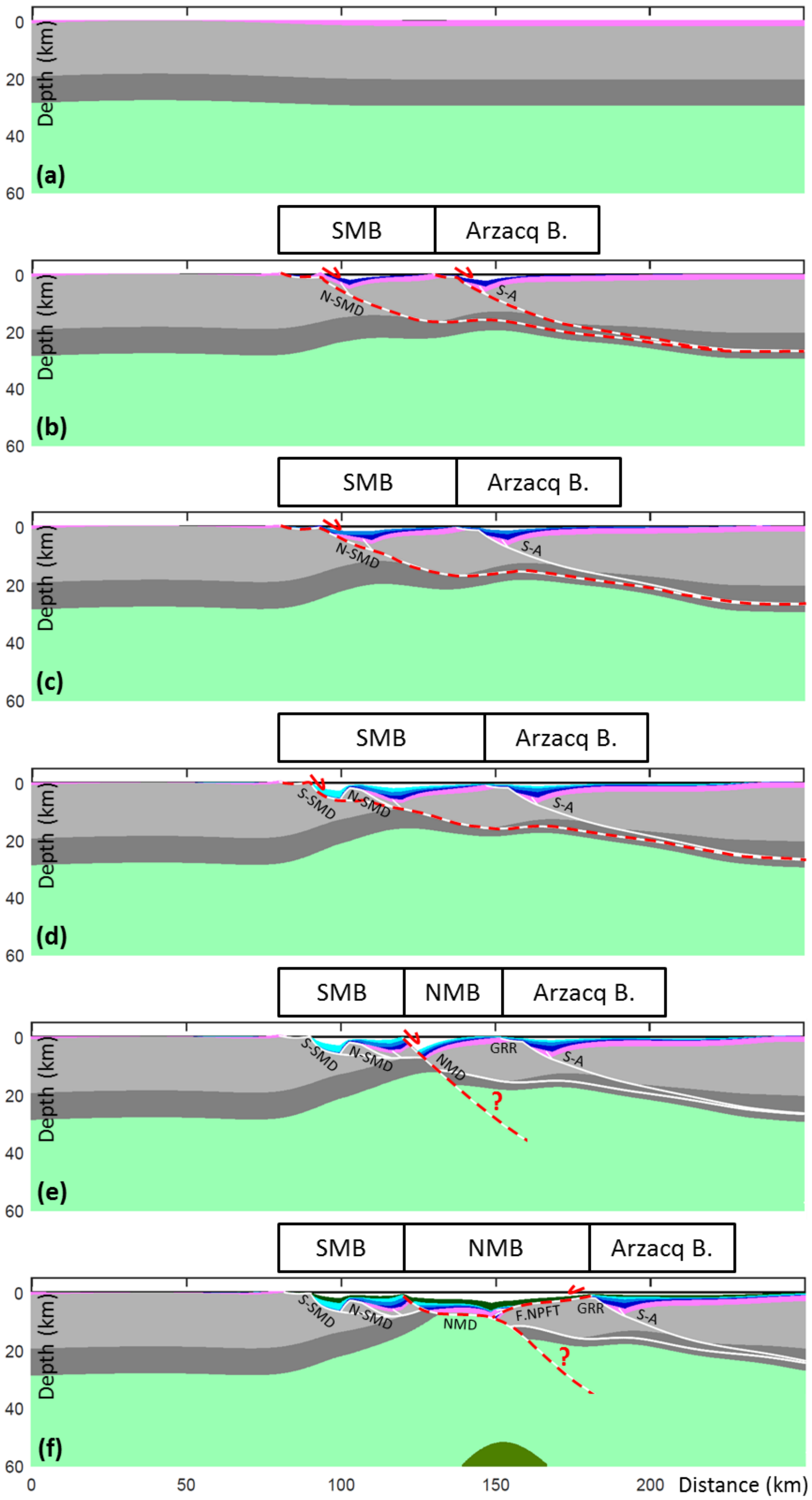

Figure 7: Detail of the rifting evolution of the Western Pyrenees shown in Figure 6. Red dashed lines indicate active extensional faults whereas white solid lines are inactive extensional faults. **a)** Slight crustal thinning is achieved by lithosphere stretching and thinning. **b)** The N-SMD and the S-A extensional faults are moved at this stage. Sediments partly fill the SMB and the Arzacq Basin. **c)** The N-SMD extensional fault is re-activated at this stage and sediments added. **d)** The S-SMD extensional fault is active at this stage and sediments added. **e)** The NMD extensional fault is active at this stage. **f)** The F.NPFT is active at this stage and a new sedimentary unit fills the SMB, the NMB and the Arzacq Basin. See Figure 6 for the model legend. Structures are; **S-A:** South-Arzacq extensional fault, **N-SMD:** Northern realm of the Southern Mauléon Detachment, **S-SMD:** Southern realm of the Southern Mauléon Detachment, **NMD:** Northern Mauléon Detachment. **F.NPFT:** Future North Pyrenean Frontal Thrust, Basins: **SMB:** Southern Mauléon Basin, **NMB:** Northern Mauléon Basin and **GRR:** Grand Rieu Ridge.

Double column width **Figure 8**

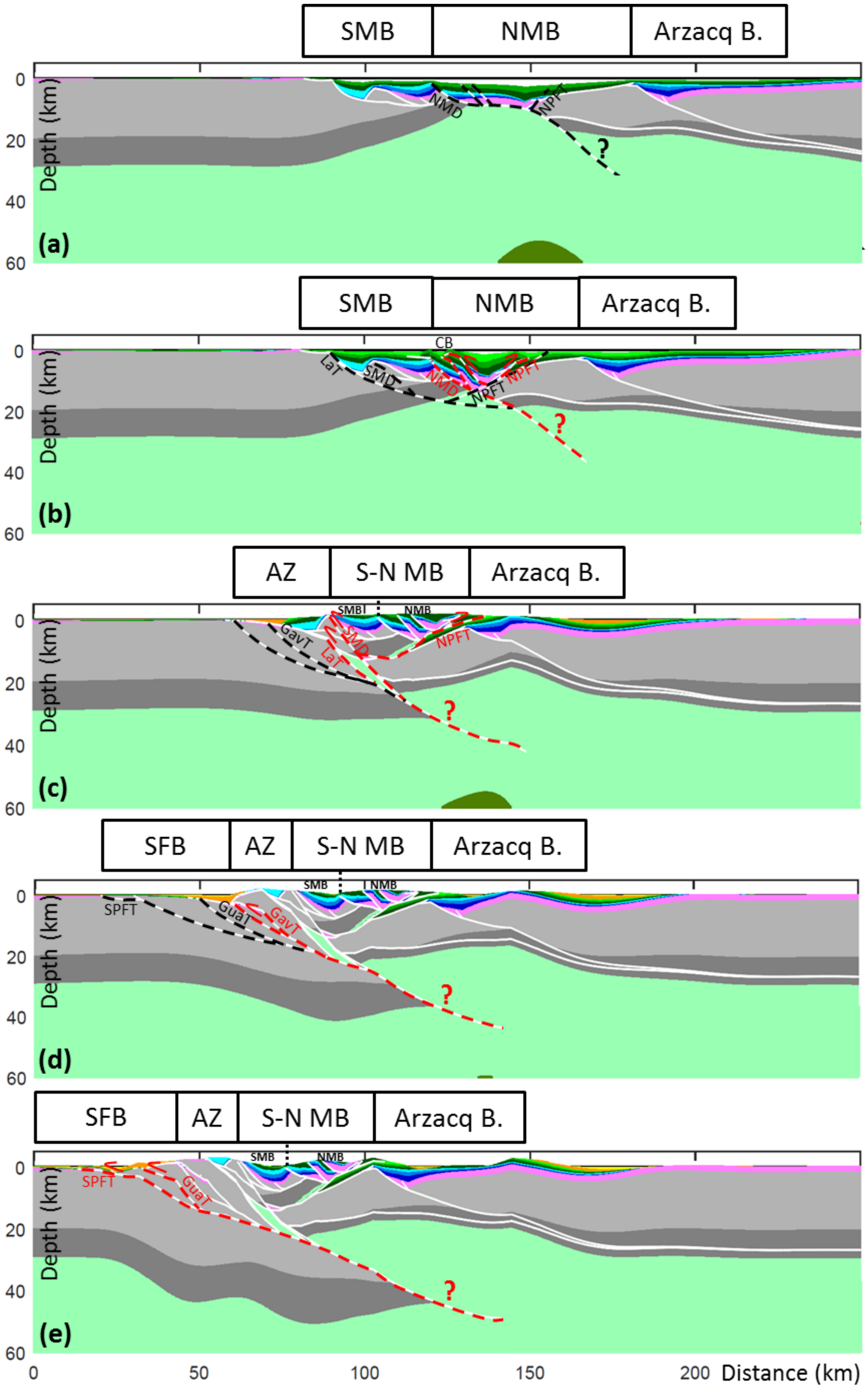

Figure 8: Detail of the orogenic evolution of the Western Pyrenees shown in Figure 6. Red dashed lines indicate active thrusts faults, black dash lines highlight the position and geometry of thrusts that are active in the next model stage and white solid lines indicate inactive faults. **a)** Pre-orogenic model stage resulting from earlier rifting and thermal subsidence. No thrusts are active at this stage however structures that will be active in the next model stage (**b**) are indicated as black dashed lines. **b)** The NMD, the NPFT and two thrusts within the sedimentary cover leading to the formation of CB are activated as thrusts. A sedimentary unit is added at this stage. **c)** The LaT system and a realm of the NPFT are activated as thrusts at this stage. A sedimentary unit is added at this stage. **d)** The GavT and a minor north-dipping thrust are active. A sedimentary unit is added at this stage. **e)** The GuaT and the SPFT thrusts are active at this stage. See Figure 6 for the legend of the models. Structures are; **NMD:** Northern Mauléon Detachment. **NPFT:** North Pyrenean Frontal Thrust. **SMD:** Southern Mauléon Detachment, **LaT:** Lakhora Thrust, **GavT:** Gavarnie Thrust, **GuaT:** Guarga Thrust, **SPFT:** South Pyrenean Frontal Thrust. **SMB:** Southern Mauléon Basin, **NMB:** Northern Mauléon Basin, **S-N MB:** Southern and Northern Mauléon Basin, **AZ:** Axial Zone, **SFB:** Southern Foreland Basin, **CB:** Chaînons Béarnais.

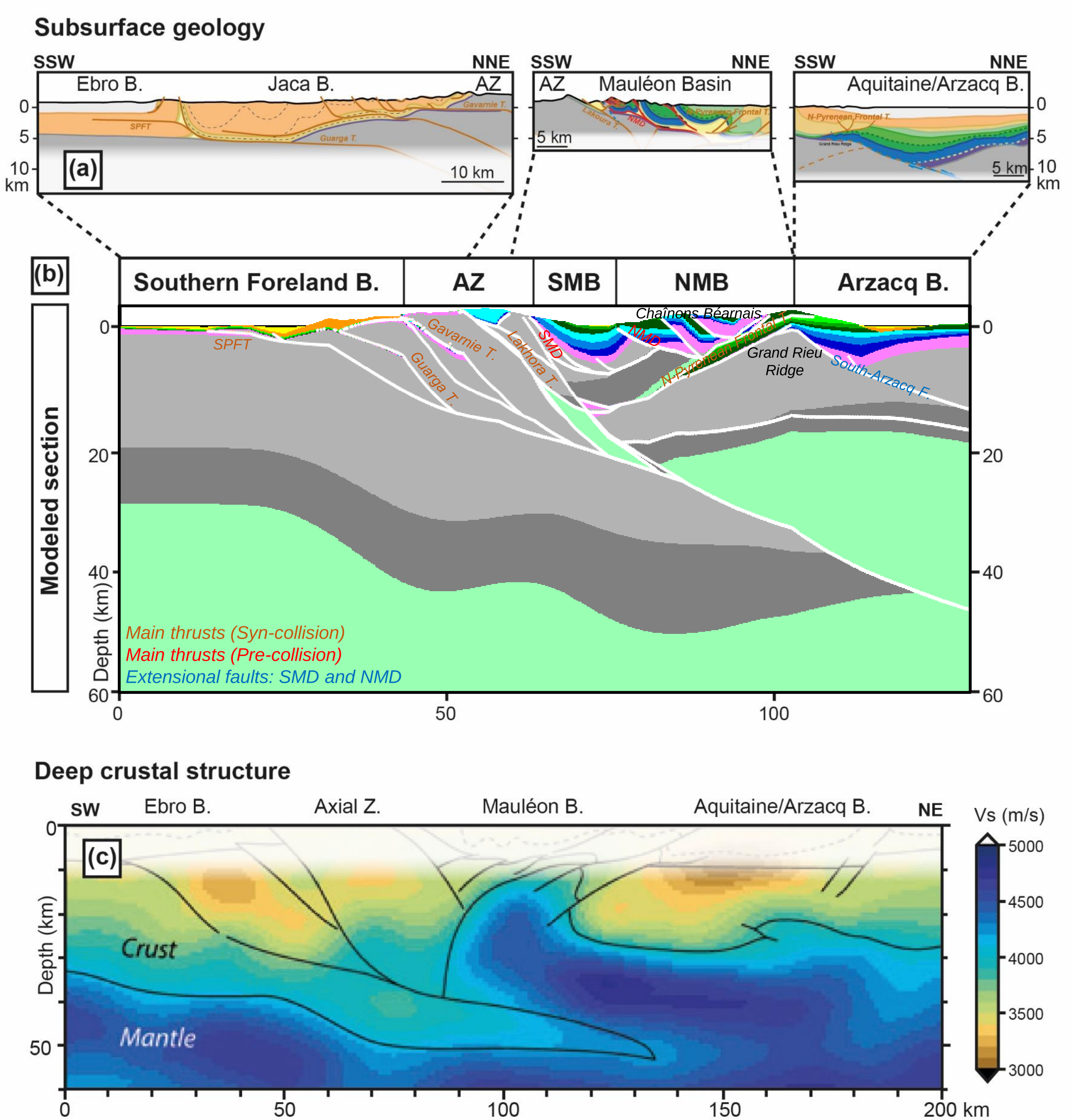

Figure 9: a) Present-day geological cross-sections across the Western Pyrenees (from South to North: after Teixell et al., 2016 and 2018; after Tugend et al., 2014; after Lagabrielle et al., 2010 and based on seismic and well data owned by Total) also shown in Figure 4 (their location is shown in Figure 2) and used as a target of the shallow architecture of the modelled section shown in **b)**. **b)** Present-day architecture of the Western Pyrenees generated using RIFTER model in this study (see Figure 6 for model legend). **c)** The PYROPE seismic transect located in the Western Pyrenees (Wang et al., 2016) and also shown in Figure 4 (its position is shown in Figure 2) used as a target of the deep crustal architecture of the modelled section shown in **b)**. **Arzacq B.:** Arzacq Basin, **NMB:** Northern Mauléon Basin, **SMB:** Southern Mauléon Basin, **AZ:** Axial Zone, **Southern Foreland B.:** Southern Foreland Basin (includes Ebro and Jaca Basins). **SPFT:** South Pyrenean Frontal Thrust, **SMD:** Southern Mauléon Detachment, **NMD:** Northern Mauléon Detachment.

Double column width **Figure 10**

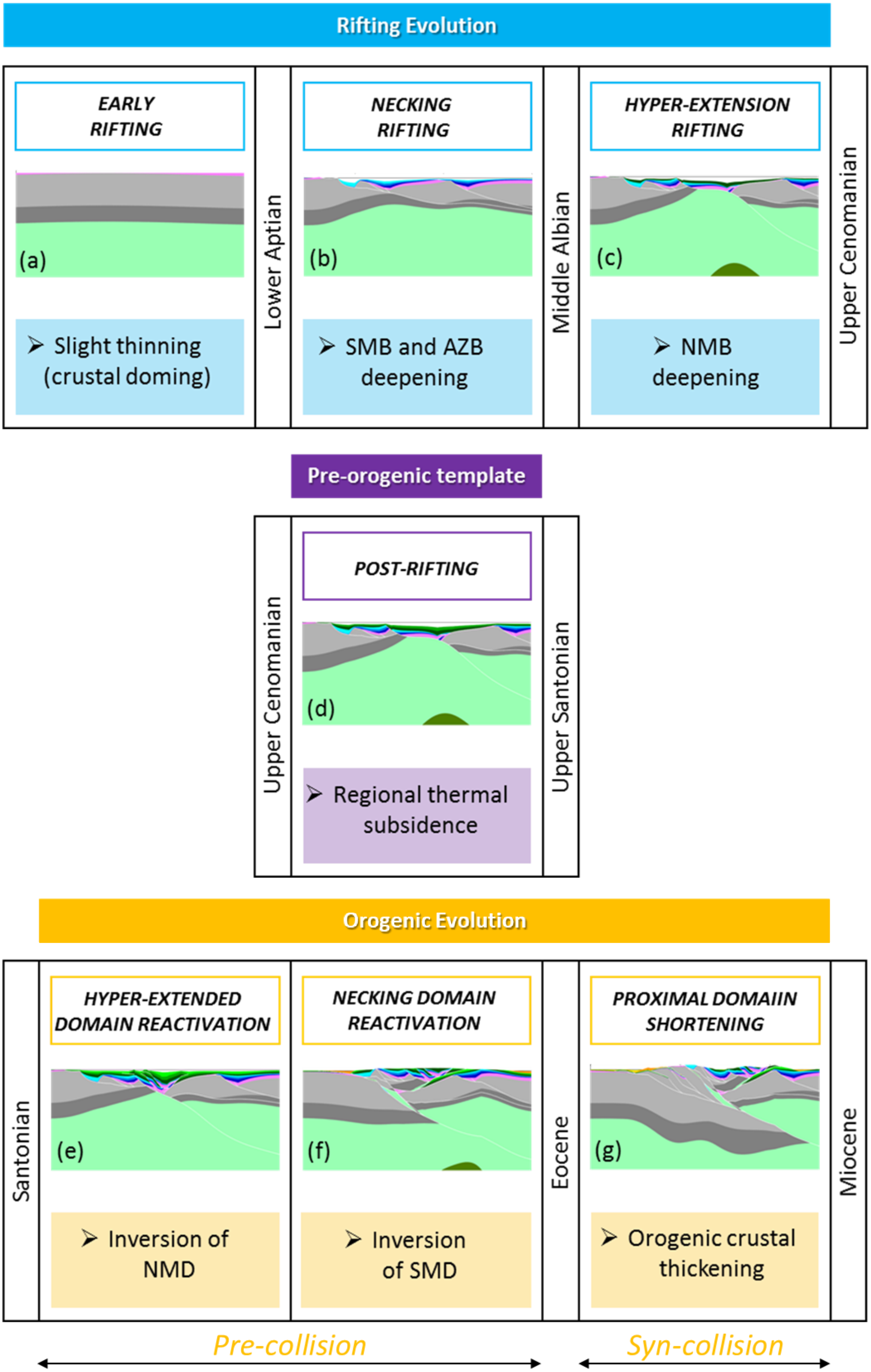

Figure 10: Evolutionary chart summarizing the rifting and orogenic evolution of the Western Pyrenees showing the different tectonic stages and their geological times. **a)** Early rifting, **b)** Necking rifting, **c)** Hyper-extension rifting), **d)** Post-rifting subsidence giving the pre-orogenic template, **e)** Hyper-extended domain reactivation, **f)** Necking domain reactivation and **g)** Proximal domain shortening. See Figures 6 models legend. Basins: **SMB:** Southern Mauléon Basin, **AZB:** Arzacq Basin, **NMB:** Northern Mauléon Basin. Structures: **NMD:** Northern Mauléon Detachment, **SMD:** Southern Mauléon Detachment.

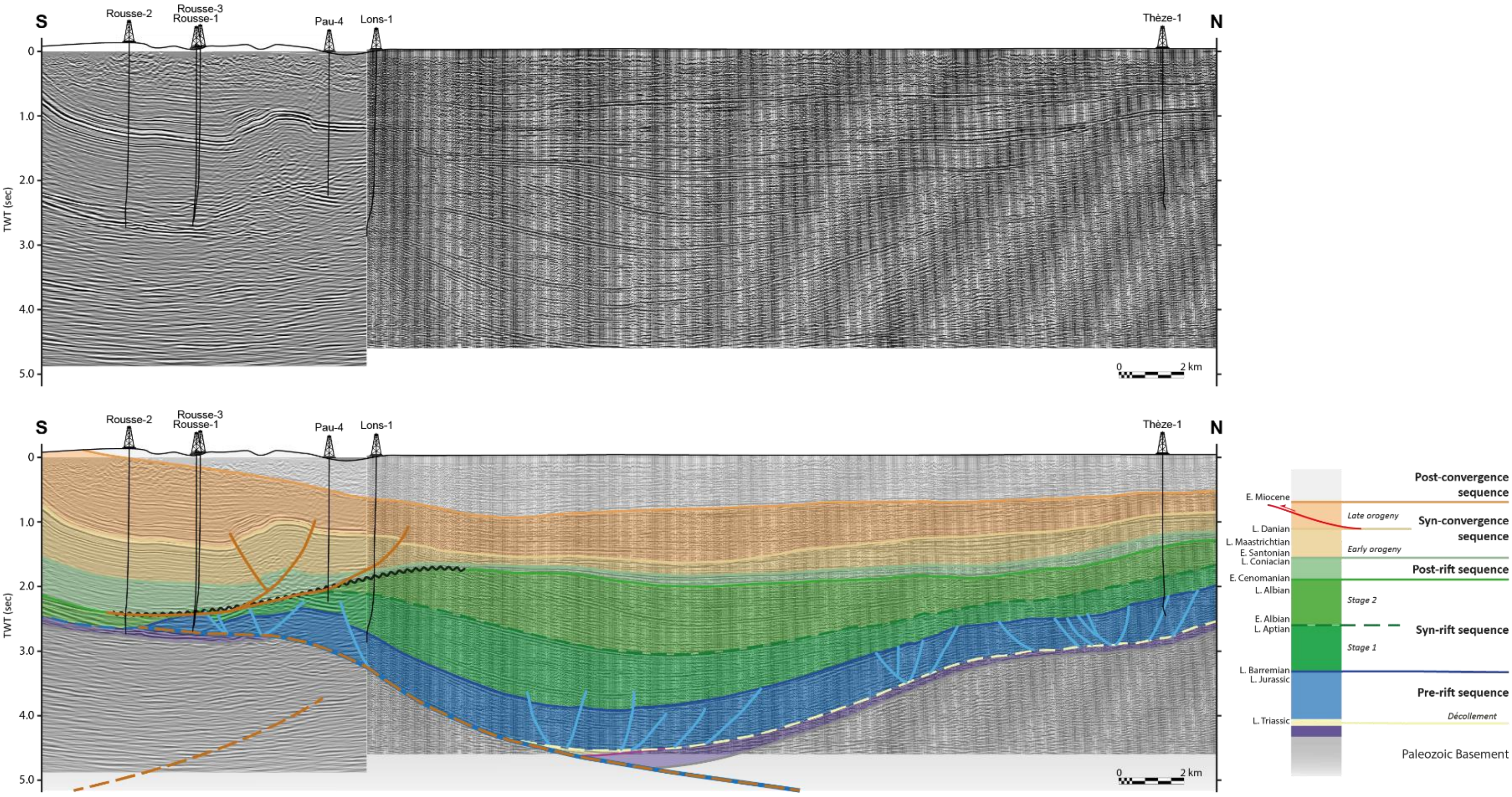

Appendix 1: Seismic line nº1325 and the position of well logs owned by Total SA (above) used to constrain the first order seismic interpretation of the Arzacq Basin (below).